Materials and Structures (2025) 58:324
https://doi.org/10.1617/s11527-025-02809-4

RILEM TC REPORT

Test methods for chloride diffusivity of blended cement pastes: a review by RILEM TC 298-EBD

Neven Ukrainczyk · Thomas Bernard · Arezou Babaahmadi · Liming Huang · Christoph Zausinger · Anthony Soive · Stéphanie Bonnet · Fabien Georget · Maruša Mrak · Sabina Dolenec · Tobias Völker · Prannoy Suraneni · William Wilson

Received: 9 May 2025 / Revised: 18 August 2025 / Accepted: 20 September 2025

Abstract The use of supplementary cementitious materials (SCM) is an important part of the roadmap for reducing CO_2 emissions and extending the service life of reinforced concrete structures. To accelerate the adoption of SCMs, the RILEM Technical Committee 298-EBD evaluates scaled-down cement paste test methods to assess the effect of SCM on resistance to chloride and sulfate ingress and reactivity, which are critical to concrete durability. This review focuses on methods for measuring chloride diffusivity and is divided into four sections: diffusivity models and parameters, diffusion test methods (including NMR and chloride measurements), migration test methods and implications for future research. Key insights highlight the complexities of multi-species ionic and molecular diffusion/migration, including various binding interactions, and compares the different measurement methodologies. The review also addresses the test scale and aggregate effects, noting the pros and cons of testing at the paste, mortar, and

This paper has been prepared by RILEM TC 298-EBD working group four (WG4) titled 'Transport with and without reactivity'. The paper has been reviewed and approved by all members of the TC.
Chair: Prof. William Wilson
Deputy Chair: Prof. Prannoy Suraneni
TC active members: Adeolu Adediran, Alana Pacheco, Alexandre Ouzia, Alisa Machner, Anthony Soive, Arezou Baba Ahmadi, Burkan Isgor, Chandra Sekhar Das, Christian Paglia, Christoph Zausinger, Chunyu Qiao, Claudiane Ouellet-Plamondon, Dhanush Sahasra Bejjarapu, Didier Snoeck, Diego Jesus De Souza, Douglas Hooton, Fabien Georget, Ilda Tole, Jason Weiss, Karen Scrivener, Klartjee de Weerdt, Kunal Krishna Das, Laetitia Bessette, Laurent Izoret, Ye Li, Liming Huang, Lupesh Dudi, Mahipal Kasaniya, Marusa Mrak, Matthieu Bertin, Mette Geiker, Mohsen Ben Haha, Neven Ukrainczyk, Prannoy Suraneni, Priyadarshini Perumal, Qiang You, Qiao Wang, Ramesh Gomasa, Reza Homayoonmehr, Riccardo Maddalena, Ruben Snellings, Sabina Dolenec, Sabine Kruschwitz, Shiju Joseph, Sofiane Amroun, Stéphanie Bonnet, Talakokula Visalakshi, Thomas Bernard, William Wilson, Wolgang Kunther, Xuerun Li, Yuvaraj Dhandapani

N. Ukrainczyk (✉)
Institute of Construction and Building Materials, TU Darmstadt, 64287 Darmstadt, Germany
e-mail: ukrainczyk@wib.tu-darmstadt.de

T. Bernard · W. Wilson
Department of Civil and Building Engineering, Université de Sherbrooke, Sherbrooke, Canada

A. Babaahmadi · L. Huang
Architecture and Civil Engineering Department, Chalmers University of Technology, Gothenburg, Sweden

C. Zausinger
Department of Materials Engineering, TU Munich, Munich, Germany

A. Soive
Cerema, Univ Gustave Eiffel, UMR MCD, 13100 Aix-en-Provence, France

S. Bonnet
Nantes Université, École Centrale Nantes, CNRS, GeM, UMR 6183, 44600 Saint-Nazaire, France

Published online: 04 November 2025

concrete scales. The review underscores the need for further investigation into testing protocols and the influence of SCM on chloride diffusion, emphasizing that comprehensive testing across different scales provides complementary information for assessing durability performance.

Keywords Chloride ingress · Diffusion tests · Migration test · Cement paste · Concrete · Supplementary cementitious materials (SCM)

Abbreviations

Shorthand notations	μXRF	Micro X-ray fluorescence spectroscopy
AFm		Alumino-Ferrite mono-substituted calcium hydrate phases (general formula $[Ca_2(Al,Fe)(OH)_6]\cdot X\cdot yH_2O$, where X is OH^-, $½SO_4^{2-}$, $½CO_3^{2-}$, Cl^-…)
AFt		Alumino-Ferrite tri-sulfate calcium hydrate (Ettringite)
BA		Biomass ash
CB		Crushed brick
CBI		Chloride binding isotherm (conventional on powders)
CC		Calcined clay
EDL		Electrical double layer
EDS		Energy dispersive X-ray spectroscopy
EPMA		Electron probe micro-analyser
FA		Fly ash
GGBFS		Ground granulated blast-furnace slag
HTO		Tritiated water
ICP		Inductively-coupled plasma
LIBS		Laser-induced breakdown spectroscopy
LA		Laser ablation
LL		Limestone filler
PC		Portland cement (OPC – ordinary portland cement)
MS		Mass spectrometry
PIXE		Particle-induced X-ray emission
PLC		Portland cement blended with limestone
RCM		Rapid chloride migration
RT		Reactive transport
SCM		Supplementary cementitious materials
SSA		Sewage sludge ash
TD		Thermodynamics (Chemical equilibrium)
TXM		Transmission X-ray microscopy
Mathematical parameters	C_S	Total chloride concentration at the specimen surface (exposed to chloride solution)
	C_d	Total chloride concentration at penetration depth x_d where colour changes in a colorimetric method
	D	A diffusion coefficient in general terms
	D_0	Self-diffusion coefficient (tabulated values for infinite dilution in water) related to random molecular motion in the absence of a concentration gradient

F. Georget
Institute of Building Materials Research, RWTH Aachen University, Aachen, Germany

M. Mrak · S. Dolenec
Slovenian National Building and Civil Engineering Institute, Ljubljana, Slovenia

S. Dolenec
Department of Geology, Faculty of Natural Sciences and Engineering, University of Ljubljana, Ljubljana, Slovenia

T. Völker
Federal Institute for Materials Research and Testing, Berlin, Germany

P. Suraneni
Civil and Architectural Engineering, University of Miami, Florida, USA

D_{app}	Apparent diffusion coefficient (vague usage, typically referring to combined chemical and physical nature)
D_{F1}	A general diffusion coefficient used in Fick's first law
D_{eff}	Effective diffusion coefficient (vague usage, typically referring only to theoretical physical morphological nature) driven by concentration or activity gradients
D_{intra}	Intraphase diffusion coefficient of a species within a specific phase (e.g., water, solution, pore solution) driven purely thermally, or by specific gradients
D_{inter}	Interdiffusion (or mutual diffusion) coefficient due to a net movement of multiple species driven by concentration gradients
D_{ssm}	Steady-state migration diffusion coefficient
D_{ssd}	Steady-state diffusion coefficient
D_{nssd}	Non-steady-state diffusion coefficient
D_{nssm}	Non-steady-state migration diffusion coefficient
P	Porosity
w/b	Water-to-binder mass ratio
w/c	Water-to-cement mass ratio
x_d	Penetration depth where colour changes in a colorimetric method

1 Introduction

The use of supplementary cementitious materials (SCM) can reduce CO_2 emissions by partially replacing cement and extending the service life of reinforced concrete structures. For durability [1], it is important to understand how SCMs influence long-term chloride ingress in cementitious materials [2], a focus of the RILEM Technical Committee 298-EBD. The committee evaluates down-scaled cement paste test methods to assess SCM effects on resistance to chloride and sulfate ingress which significantly impact concrete structures durability. The committee is divided into four sub-working groups: WG1 – Microstructure, WG2 – Reactivity with chlorides, WG3 – Reactivity with sulfates, and WG4 – Transport with and without reactivity. WG4 aims to evaluate cement paste test methods to quantify the effects of new SCM on transport-diffusivity properties related to chloride (and sulfate) ingress. The term 'reactivity' refers to two aspects: 1) chloride binding reactions and 2) ongoing hydration of cement and SCM. 'Without reactivity' pertains to purely diffusive mechanisms in inert porous media, excluding concurrent binding and hydration. To study chloride ingress in concrete, standard methods like bulk diffusion or accelerated migration tests have been developed. This review concentrates on various experimental methods to obtain a diffusion coefficient D derived from chloride (flux or profile) measurements (Table 1). Chloride flux measurements are relevant for steady state through diffusion tests, typically measuring changes in the exposure solution, while non-steady-state methods involve solid profile measurements. Shi et al. [2] reviewed existing methods, discussing pros and cons. Recent work (e.g. [3]) showed that scaling diffusivity tests to cement paste reduces variables, labor and testing time. The overall goal of the subgroup 4 is on evaluating these scaled-down methods to assess SCM effects on cement paste's resistance against chloride ingress.

This review paper is organized into four main sections to systematically address chloride diffusivity in cementitious materials.

2 Chloride diffusivity models and key parameters

To avoid confusion, it is crucial to clearly define various forms of diffusion coefficients (D's) using the models and/or experiments utilized to derive them. Chloride ingress in cementitious materials can be mathematically described using modelling approaches of different complexities. The service life extrapolation capability is strongly affected by the

Table 1 Common standard methods to measure ionic diffusivity in concrete, along with related sections in the structure of the current paper, the measured parameters and selected references to standards and/or reference papers

Category	Short description	Section	Parameter	Standards (or reference papers)
Diffusion	Self-diffusion	3.1	D_0, D_{intra}	[4, 5]
	Steady state through diffusion	3.2	D_{ssd} (D_{eff})	None [6]
	Non-steady-state bulk diffusion	3.3	D_{nssd} (D_{app})	ASTM C1556 [7], NT build 443 [8], ISO 1920–11 [9], EN 12390–11 [10]; Chloride profiles by NT Build 208 [11] or more detailed RILEM recommendations [12, 13]
Migration	Steady state	4.1	D_{ssm}	NT Build 355 [14], XP P 18–461 [15]
	Non-steady-state (RCM)	4.2	D_{nssm}	NT BUILD 492 [16], French XP P 18–462 [17], EN 12390–18 [18], Spanish UNE 83987 [19] and UNE 83992–2 [20]

level of model simplification. Simple chloride (and carbonation) ingress models are empirical single-species analytical solutions of diffusion equations mainly for curve-fitting [21–23]. More complex models [24], such as reactive transport multi-species approaches [25–27] require a reliable diffusion coefficient (D_{eff}), chloride binding and other reaction mechanisms as key input parameters.

Scaling laboratory D values to field conditions remains a key challenge in predicting concrete's long-term durability. The accelerated lab experimental results, typically obtained in weeks (or days), have limited value to extrapolate the service-life of concrete structures [22, 28]. Thus, a better understanding of the combination between modeling and various lab experimental methods available to obtain D parameters is of critical importance. Extrapolations based on scientific principles and calibrations using such (accelerated) datasets, could significantly enhance the accuracy of service-life predictions. Here, complications due to missing data and methodologies on how to evaluate the effects of SCM on the chloride ingress, makes the search for adequate models and input parameters even more relevant.

2.1 Parameters influencing chloride diffusivity

Chloride ingress in concrete involves multiple interacting factors, including concrete-scale effects, chloride binding, porosity, pore solution and environmental conditions (Fig. 1). Decoupling these parameters is essential for understanding mechanisms and enabling long-term performance prediction. Without Cl binding, the diffusion of substances in hydrated cement paste is primarily controlled by the interconnected capillary pores, influenced by factors like water/binder ratio, binder (degree of) hydration, and material properties. Pozzolanic and hydraulic SCMs enhance binder pore connectivity and tortuosity (including pore constrictivity), reducing diffusivity. However, inadequate curing, especially with SCM and low water/binder ratios, can lead to insufficient hydration near surfaces, increasing D. Air voids, porous aggregates, and aggregate-paste interfaces also impact diffusion pathways. Effects of hydration reactivity, chloride binding, binder and pore solutions chemistries are discussed by Weerdt et al. [23]. The influence of both material-related and environmental factors on chloride diffusivity in concrete is summarized in Table 2, highlighting key parameters such as water-to-binder ratio, SCM use, pore structure, temperature, and relative humidity.

2.2 Empirical and more deterministic model approach

2.2.1 Model based on D_{app} (D_{nssd}, D_{nssm})

Shafikhani et al. [29] reviewed analytical (mostly empirical) mathematical models for concrete chloride diffusion, based on tests for D_{nssd} and D_{nssm}, analyzing a wide range of experimental data, including SCM effects (silica fume, fly ash, slags, limestone) with various cement replacement dosages, as well as the aggregate volume fraction, cement content and max aggregate size. Results show that models incorporating capillary porosity, pore structure, diffusivities, aggregate volume, and ITZ properties deliver the highest accuracy and precision. Some models have used D_{app} derived from bulk diffusion tests without explicitly accounting for chloride binding [7], while others used D_{eff}, incorporating chloride binding

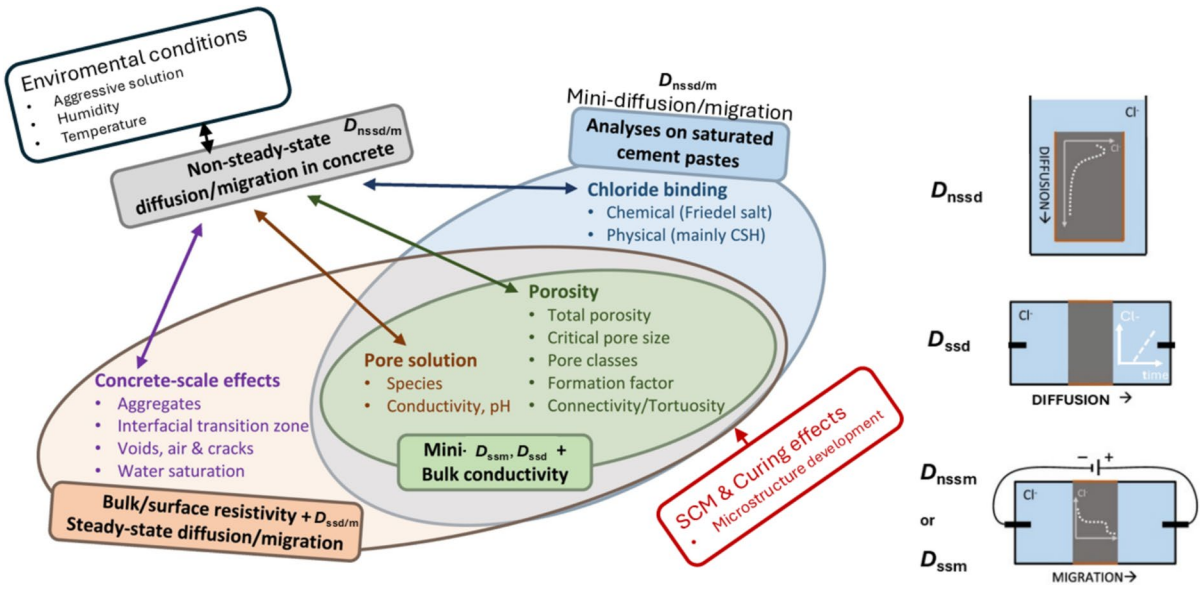

Fig. 1 Key parameters of chloride ingress included in the different types of experimental tests at different scales

Table 2 Key parameters affecting chloride diffusivity in concrete

Parameter type	Category	Specific factor	Rationale/impact
Material	Water-to-binder ratio	Low w/b ratio	Reduces pore connectivity; lowers diffusivity
	SCMs (e.g., slag, fly ash, calcined clays)	Alters binding (↑AFm), lowers pH, refines pores	Enhances chloride binding; affects pore solution composition
	Clinker dilution	Less C-S–H formed	Reduces binding capacity
	Aggregate design	Optimized content and grading	Reduces tortuosity, improves barrier effect
	Air voids	Controlled air content	Saturation-sensitive voids influence transport
	Cracking	Minimized cracking	Cracks create fast paths for chloride ingress
	Pore morphology	SCMs refine pore size distribution	Smaller, disconnected pores hinder diffusion
	Chloride binding	Strong chemical (AFm) & weak physical (C-(A-)S–H) binding	Buffers free Cl^-; impacts total transport
	Donnan exclusion	Ion exclusion in small pores	Lowers effective diffusivity
Environmental	Exposure solution	Use realistic ions (e.g., seawater, $CaCl_2$)	Affects binding chemistry and transport
	Temperature	Control ambient/curing temperature	↑T significantly increases diffusion rate
	Leaching effects	NaCl diffusion, OH^- buffering	Alters pore chemistry, pH, and ionic strength
	Relative humidity	Partial saturation (RH < 100%)	Reduces continuity of water phase; lowers mobility

corrections, typically based on migration test data. Combined analytical and numerical multi-scale modeling provide a novel perspective to study the chloride penetration in concrete by considering the effects of both the multi-scale microstructural characteristics and multi-species interactions [29].

The commonly used D_{app} (Fick's 2nd) approach Weerdt (2023) [23] is an empirical parameter obtained by fitting concentration profiles to simplified (diffusion-like) models that lump together the diffusion mechanisms with mechanisms not explicitly included in the model [21, 22]. This engineering approach, used in many studies on site after long exposure to sea water [30, 31], reduces model complexity and the number of parameters, it may significantly limit the model's extrapolation

capabilities, especially under nonlinear concentration dependencies.

2.2.2 Model based on D_0 or D_{eff}

Tang [32] proposed a simple analytical model to describe the main electro-chemo-physical processes of chloride diffusion in cementitious materials. It is based on the binary (single salt) electrolytic solution diffusion theory. This laid a theoretical background for the chloride ion diffusion and migration processes, linking a pure electrolyte solution theory, from diluted to concentrated systems and extending it to concrete. In this paper, the use of mathematical expressions is limited to a bare minimum, by adapting Fick's first law using appropriate correction factors [33]. This approach adapts simple models, valid for ideal cases (e.g. Fick's diffusion), to more realistic scenarios by introducing physically meaningful correction factors (e.g. for activity dependencies). The D_{F1} used in Fick's first law (Eq. 1), could be related to the flux (J) in concentrated pore solution defined by the gradient of chemical potential (or concentration c in ideal case) and D_0 (an ideal reference case for self-diffusion) through a set of coefficients (Eq. 2) [34]:

$$J = -D_{F1}\nabla\mu \cong -F_f D_0 \nabla c \quad (1)$$

$$F_f = f_\gamma f_E f_f f_p \quad (2)$$

The overall coefficient F_f should (separately) account for the different chemo-physical phenomena responsible for the non-linear dependence of the D_{F1} on the concentration (composition) of the solution (f_f f_γ $f_{E,solution}$) including surface charge effects ($f_{E,surface}$) as well as the geometrical pore structure (f_p). Briefly, f_γ accounts for activity non-ideality, f_E for the electrical coupling (e.g. as a simplification of the Nernst-Planck equation [35] and effects of surface charges) that result in relative anion/cation mobility, and f_f accounts for friction effects in concentrated electrolytes. To address solid surface charge (Donnan) effects on electrolyte diffusion, a well-established analytical steady-state theory by Revil [36] could be employed, while transient models are needed to capture coupled dynamic processes including chloride binding.

In common terminology, D_{eff} emphasizes pore geometry—related to D_0 (ideal self-diffusion), open porosity (P), and pore morphology—as the dominant factor. It can be expressed as $D_{eff} = P\ D_0\ \delta/\tau^2$, where δ (pore constrictivity) and τ (tortuosity) have solid statistical physical foundation [37, 38]. However, this approach, even at steady state, often overlooks the ionic and concentration dependency of diffusion. Without considering SCM effects, Patel et al. [39] compared f_p values, which they defined as a relative diffusivity (D_0/D_{eff}), thus neglecting all other correction factors (Eq. 2). The f_p values were correlated using exponential relationship with capillary porosity P; roughly ranging from 3 10^{-4} to 0.5 for $P = 0$ to 0.6, respectively. Systematic deviations of the trends were observed depending on the type of the test method used to estimate the D_{eff}. However, those deviations are not necessarily due to the ideality simplification, but also Nernst-Planck simplification (Eq. 2) [32]. Practically, D_{eff} is commonly related to electrical conductivity measurements via Nernst-Einstein equation [40], with porosity and pore solution chemistry contributions [41]. However, if one considers D_{eff} as typically related only to the pore structure, neglecting other relevant factors (Eq. 2), this also makes it an apparent (empirical) parameter before even considering binding (and transient coupled) effects. As demonstrated in [33] although the pore geometry is a dominant factor, it is not the only one, and does not consider the concentration dependency of D. This might explain the obtained differences of the obtained f_p values and trends as a function of OPC porosity by Patel et al. [39] For blended cements, neglecting the non-ideality (concentration, chemistry) dependence of D_{eff} could have similar consequences as for D_{app}, making them not comparable due to dependency on measurement duration and test conditions, binding, etc., when considering changes in binder (SCM) chemistry.

Concentration dependence of D_{eff} can be described using the intrinsic friction parameter ψ, as per Tang's model. This model has been recently refined [33] by calibrating the pore geometry factor (f_p, Eq. 2) using same D_{ssd} measurement data for OPC. A novel method to estimate ψ in OPC materials accounts for better separation of parameters, showing ψ to be 1.9 times higher than in pure NaCl solutions, significantly lower than Tang's values. This study systematically examines factors affecting D_{ssd} chloride concentration dependency, highlighting D_{ssd} test as a promising but time-intensive to understanding SCM effects.

Advanced (multi-component) reactive-transport models present a significant challenge as various mechanisms are interlinked, making it highly challenging, if not impossible, to independently obtain the required model parameters. For instance, the coupling of Cl binding with D through multi-ion and surface-EDL interaction models leads to the emergence of more fundamental (intrinsic) D. The proposed simplified relations (e.g., D_{nssd} vs. D_{ssd}) operate under the assumption that certain effects, such as chloride binding, can be eliminated in steady-state diffusion tests. Performing tests with multiple upstream concentrations facilitates the determination of both the intrinsic D_{eff} (though still away from its oversimplistic physical meaning), which only better approaches the true effective diffusivity coefficient at zero concentration extrapolation, and the concentration dependency of D_{ssd} in relation to Cl-salts.

2.2.3 Relationships between diffusion coefficients

Many simplified relationships between the various D's are proposed in literature, and their limitations should be made clearer. D_{nssd} (D_{app}) is typically (over) simplified by relating it to the D_{ssd} (D_{eff}), porosity and chloride binding isotherm: e.g. $D_{nssd} = D_{ssd} / (P + dC_b/dC_f)$. Note that the binding term is constant only if the isotherm is linear [21, 42]. Analytical relations between the diffusion coefficients were established by Tang [32], based on 1:1 electrolyte theory of diffusion. For example, the link between D_{ssd} and D_{ssm} depends on the Cl binding, concentration (dD_{ssm}/dc) and potential gradient. However, how to consider such parameters quantitatively remains a key challenge. If neglecting binding in the (short transient) migration test, the following relation is suggested $D_{ssm} = P\ D_{nssm}$ [43], however only as a crude first approximation as binding and other effects in migration are still unclear.

2.2.4 Effect of aggregates

Several studies in the literature show that beyond 50% by mass of aggregates a continuous pathway is formed between the ITZs of each aggregate (Winslow et al., 1994) and that most of the cement paste is ITZ [44, 45]. Although controversial today for concrete, this conclusion seems appropriate for mortars for which the quantity of aggregates is significant in volume percentage. By neglecting the water adsorption capacities of the aggregates (assuming the aggregates are saturated with water) and by assuming a negligible diffusion rate in these same aggregates, Soive et al. [46] showed that the diffusion of chloride ions in a mortar can be the result of the diffusion in cement paste plus the geometrical effect of aggregates. Although these results were obtained on Portland cement-based materials, they suggest that the tests on cement paste can be transposed to mortars, the transition from mortar (or cement paste) to concrete being worth exploring, particularly in the presence of SCM.

So, there is a broad range of different models which require different inputs and have different definitions of diffusion coefficients. The available methods for each D at different scales are presented in the following sections.

2.2.5 Chloride binding models

Chloride binding in cementitious materials is typically described using linear, Langmuir, or Freundlich isotherm models [23, 27, 47, 48] which relate (using direct analytical expressions) the concentration of bound (or total) chlorides to the free chloride concentration in pore solution. More fundamental approach is based on thermodynamic (numerical) modelling [24–26] that predicts pore solution properties, solid–solution interactions (e.g., hydration, pozzolanic reactions, chloride binding), and supports advanced reactive transport modeling with minimal experimental inputs [48]. Kinetic expressions for chloride binding have also been proposed [47]:

$$\frac{dC_b}{dt} = k_b\left(C_{beq} - C_b\right) \tag{3}$$

where C_b is the current bound chloride concentration, C_{beq} is the equilibrium bound chloride concentration, k_b is the chloride binding rate constant (3.13×10^{-7} m^3/mol/s). When $C_b > C_{beq}$, chlorides desorb; when $C_b < C_{beq}$, free chlorides are bound.

Chloride binding is affected by the w/c, tricalcium aluminate and SCM type, pore solution chemistry, and replacement amounts [48, 49]. Generally, SCM changes the chloride binding; less physical binding [23, 50], with available alumina being considered the factor that leads to the most chemical binding, due

to the formation of greater amounts of Friedel's salt [51]. Kinetic factors and slow evolution of the microstructure must be accounted for in SCM mixtures, and many such corrections (e.g. aging factors) are available in literature [22] [52–55].

3 Diffusion tests

3.1 Self-diffusion experiments

Molecular or ionic self-diffusion (Table 3) represents the autonomous movement of molecules or ions within a substance, propelled solely by the inherent randomness of thermal motion. Intraphase diffusion is driven purely thermally, or by specific gradients. In contrast, inter-diffusion arises from concentration (chemical potential) gradients, leading to the blending of different molecules or ions upon contact. Both self-diffusion and intra-diffusion differ from ionic mobility, which results from external forces like an electrical potential gradient. The Nernst–Einstein relationship establishes a connection between the coefficients of self-diffusion and mobility. Diffusion is intricately affected by concentration. Molecular size and interactions, including attractive or repulsive forces, also influence diffusion. Additionally, increased ionic strength impedes diffusion due to enhanced electrostatic interactions among ions.

3.1.1 Field gradient nuclear magnetic resonance (FG-NMR) method

FG-NMR provides D_0 (or D_{intra}) coefficients of molecules and ions, like chloride, by tracking their random motion using pulsed magnetic field gradients (PFG), without the need for a tracer [4, 56]. These gradients encode spatial information into the nuclear spins. As molecules diffuse, they experience phase shifts in the NMR signal. By analysing signal attenuation with respect to the applied field gradient and diffusion time, the diffusion coefficient is calculated. However, the FG-NMR method is typically limited to the early hydration stages of white cements that are very low in paramagnetic impurities (like Mn- and Fe-oxides).

Nestle [4] reviewed NMR studies on self-diffusion in hydrating cement pastes, noting that diffusion studies are less common due to their complex NMR setup requirements, unlike the more prevalent relaxometry studies with simpler setups. Hansen [57] studied long-range diffusivity by PFG NMR (< 1s) and validated it versus D_2O-H_2O (> h) exchange. The study was done on white cement, and proposed an analytical solution with two *D's* (within the cement sample and in external solution) to fit the NMR results. Analytical

Table 3 Definitions and comparison between self-diffusion (D_0), intra-diffusion (D_{intra}), and inter-diffusion (D_{inter}), in both homogeneous water (solution) and porous media ('inert' concrete)

Aspect	D_0 (Self-Diffusion)	D_{intra} (Intra-Diffusion)	D_{inter} (Inter-Diffusion)
Definition	Random motion of identical molecules/ions without a gradient	Diffusion of a species within a specific phase (e.g., water, solution, pore solution)	Net movement of multiple species driven by a concentration gradient
System	Single component in homogenous systems	Multi-component systems, focusing on diffusion in one phase	Multi-component systems, with interaction between species
Driving Force	Random thermal motion (Brownian motion)	Random motion (or specific gradients)	Concentration or chemical potential gradient
In Homogeneous Water	Free diffusion of molecules; highest diffusion coefficients due to no restrictions	Like self-diffusion; minor differences due to interactions	Interaction between species (e.g., Na^+ and Cl^- in saltwater)
In Concrete (Porous Media)	-	Constrained within a specific phase, with additional effects from pore geometry and interactions	Complex mixing behavior across phases; further reduced by confinement
Measurement Methods	FG-NMR, tracer-free techniques	FG-NMR, isotopic or chemical tracers (for specific species)	Tracer techniques, diffusion couples, or profile analysis

solutions in [5, 56] considered more common (single D approach) and different diffusion geometries and changing (heavy-water-to-water volume ratio) boundary conditions.

Benefits of NMR methods are in elimination of binding interactions artefacts with cementitious solids, as the binding of proton and deuterium water can be neglected, i.e. it enables the calibration of geometrical pore structure, f_p in Eq. 2 and 1. NMR measurements, which may take from up to 2 weeks, are still > ~3 times shorter than single (salt) concentration through-diffusion steady-state measurements. However, they are expensive, and FG-NMR measures self-diffusion, which is an average distance travelled by diffusing molecules due to thermal motion in a chemically uniform environment. Inter-diffusion, a more relevant process driven along a concentration gradient involves a tracer (e.g. ^{2}H or ^{18}O) diffusion approach, where NMR may be used to measure the concentration changes.

Simple NMR techniques are employed to measure the concentration change during an intra-diffusion process [5]. An inside-out diffusion setup involves following the exchange between water inside the sample with an external deuterium water solution. The intra-diffusion coefficient is obtained by fitting the diffusion model's analytical solution to the measured transient change of the sample's total water concentration. This method is valuable for water-saturated porous media with short relaxation times (< 1 ms), making it suitable when conventional NMR pulsed field gradient techniques are impractical. Implementation is straightforward, requiring only the recording of a free induction decay (FID) or Hahn echo [4] ,56, 58.

In Fleury's 2020 study [58], diffusion coefficients were examined in CEM I and V paste, mortar, and concrete (with and without metalic fibers) using fast ^{1}H-NMR. Deuterium-water exchange facilitated inside-out diffusion in cylindrical samples over 17–125 days. Water saturated samples were placed in NMR tubes with deuterium-water. Sample sizes were 10 mm in diameter and 15 mm in height for paste and mortar, and 20 mm in diameter for concrete. NMR magnetization signals were calibrated against known water volumes to measure proton concentration over time. Porosity was determined from additional NMR measurements, following Carr–Purcell–Meiboom–Gill (CPMG) spin-echo pulse sequence approach. The study also compared results with tracer diffusion, Magnetic Resonance Imaging (MRI), and other destructive profiling methods. The pore diffusion coefficient ($D_p = D_{eff}$ / $P_{connected}$) was calibrated using simple analytical Fick's 2nd solution for inside-out diffusion (analogous to moisture diffusion). Interestingly, porosity was not required to model transient diffusion, as NMR measures total concentration across the sample.

Fleury's study [58] found that CEM V-based materials had significantly lower D_{eff} compared to CEM I, mainly due to lower D_p and, to a lesser extent, lower accessible porosity (Fig. 2). The addition of fibers increased D_p by creating more diffusive paths, but this effect was counteracted in CEM V concrete by its much lower accessible porosity. The results

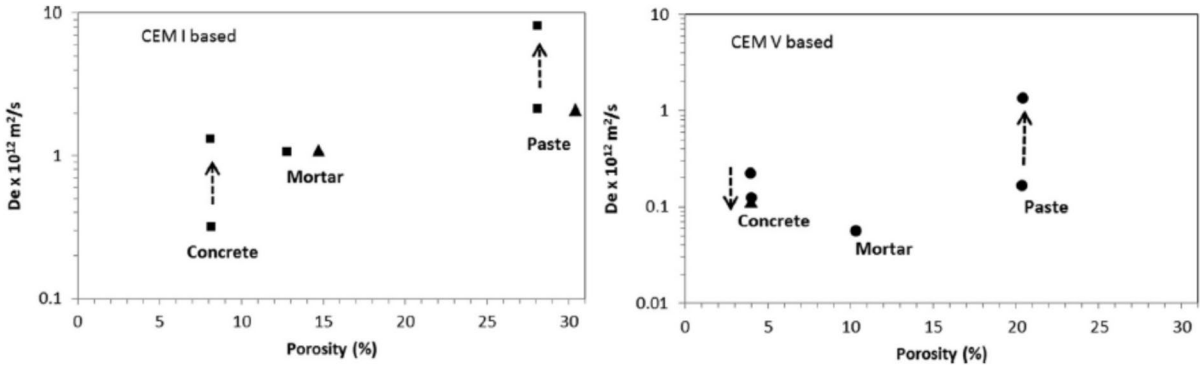

Fig. 2 ^{1}H-NMR inside-out diffusion method Fleury et al. [58] examined CEM I (left) and CEM V (right) in paste, mortar, and concrete samples. The dashed arrow indicates the inclusion of metallic fibers, while triangles indicate HTO through-diffusion validation result

showed good agreement with HTO through-diffusion measurements.

Valori et al. 2013 [59] reviewed ^{1}H-NMR experiments on cement-based materials, emphasizing the use of D as a function of diffusion time (τ_D) to unveil pore size effects. They cautioned against using the PFG method for gel pores due to size limitations and discussed challenges in cement pastes where adaptations like shorter gradient pulses and specialized sequences are needed to counter magnetic field heterogeneity and mitigate signal loss caused by short T_1 and T_2 relaxation times of pore water, reflecting rapid dephasing from strong pore surface interactions. Two-dimensional PFG variants could explore relaxation–diffusion correlations and pore anisotropy.

3.1.2 NMR tracer method

The NMR tracer method is a technique used to measure D_{intra} and D_{inter} (Table 3) in multi-component systems using NMR-active tracer nuclei (isotopically labelled) [60, 61]. This method involves introducing a small concentration of NMR-active tracer molecule/ions into a system and tracking their diffusion behavior. The tracer's movement is typically monitored using NMR or FG-NMR, to obtain its diffusion coefficient. Although specialized NMR setups are essential for coupling inter-diffusion with drying/capillary sorption, NMR remains effective for simultaneous measurement of moisture and multiple ion contents in (partly moisture saturated) porous materials [62].

3.2 Steady-state natural diffusion experiments

Steady state diffusion experiments use two compartments separated by a specimen. The first compartment contains the diffusing species of interest, which penetrates through the specimen into the downstream compartment. The steady-state diffusion coefficient (D_{ssd}) is determined by either elemental profiling along the permeated sample cross-section, measuring the diffusion potential due to charge transfer [63], or by analysing the cumulative species quantity in the downstream compartment. Once a steady increase of cumulative species quantity is reached in the downstream compartment, D_{ssd} is derived from the linear slope using Ficks's first law [39].

For diffusion of non-charged molecules like tritiated water (detailed below) provides good theoretical approximation. However, the applicability of Fick's first law to charged ions like chlorides in electrolytically active environments like pore solution in cementitious materials leads to significant deviations [64]. Moreover, binding reactions and physical interactions within the sample add further complexity. Identifying species with similar diffusion properties to chlorides but minimal interactions with cementitious ions can help mitigate these complexities.

For decades, tritiated water (HTO) has been an elaborate but precise tool for measuring diffusion coefficients of relatively inert, diluted molecules within cement-based materials. HTO involves replacing some hydrogen atoms with tritium atoms (^{3}H) which can be detected due to their radioactivity. Originally used in nuclear power plants, the long-term interaction of Tritium with cement paste (w/c = 0.4…0.55) and mortar (sand/cement = 1.25…2.25) was investigated [65] using 2.3 cm thin disks (D = 4.5 cm). Today, HTO is used for measuring diffusivity in porous materials due to the lack of significant interaction of HTO with the cementitious matrix [61]. Due to long equilibration time (months), the method is limited to (cm) thin samples, thus more appropriate for cement pastes and mortars than concrete samples. The higher variability in mortar results is attributed to specimen heterogeneity due to sand inclusions (90% d < 2.5 mm) [65].

Pure diffusion via HTO is handy and cost-effective but showed that scaling diffusivity tests to cement paste reduces variables, labor and testing time. In [66], comparative results for [39] effective diffusion coefficients of HTO in relation to prominent ions like Cl- or O_2 are analysed from 14 publications. The extensive literature review reveals nearly congruent values for the effective diffusion coefficients of HTO and chloride ions (Fig. 3).

D_{eff} of chloride ions is similar as that of tritiated water and higher than the sodium ions. This difference can be attributed to the electrical double layer near the charged C-S–H surfaces [66]. The general congruence enables further studies on diffusivity of ions like chlorides but with the benefits of being able to dispense on complex reactivity during diffusion.

Larbi et al. [61] studied the influence of aggregates on the D_{eff} in mortars using HTO diffusion, confirming the correlation between increased w/c ratio (and aggregate content) and enhanced diffusion. Similar trends were observed in hardened cement paste and

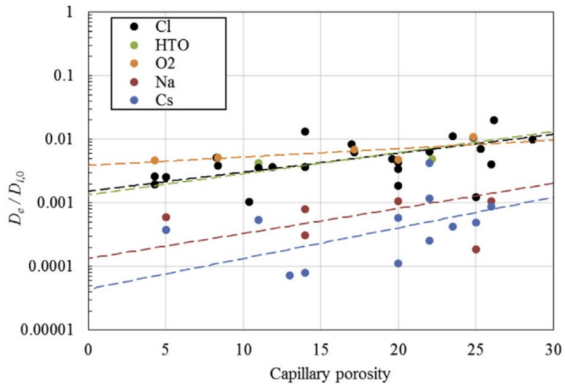

Fig. 3 Comparison of effective diffusion (relative to self-diffusion, $D_{eff}/D_{i,0}$) coefficients for different ions *i* [66]

mortars [65]. Long-term tracer HTO and Cl^{36} diffusion [60] showed reduced Cl^{36} D_{eff} within the first 1.5 years followed by a slower decrease up to 6 years. After 4 years, chloride flux measurements become unfeasible [60] in some cells (1 cm thick: 5 mm cement paste + 5 mm clay; $D = 3.5$ cm). Sammaljärvi et al. [67] performed similar studies comparing ^{36}Cl and HTO in two different concretes ($d_{max} = 1$ cm) via autoradiographic imaging of the permeated specimen ($h = 1$ cm; $D = 3.5$ cm) cross-section. They observed similar D_{ssd} of ^{36}Cl and HTO in both CEM I and CEM V concretes (binding effects should be modelled separately). HTO showed no retardation whereby the distribution coefficient of ^{36}Cl was obvious and pronounced differently between the two kinds of binders in concrete. This study shows the advantage of HTO in cementitious materials to relate the diffusion of an interactive ionic species with the non-reacting species. However, such simplifications are not true in clays. In compacted bentonite [44] HTO accessible porosity was equal to the total porosity, while the chlorides (compared to HTO) show an order of magnitude lower values and a stronger decrease in both D_{eff} and accessible porosity with increasing dry density. This difference is attributed to the ionic interaction with surface charges bentonite clay.

To sum up, HTO steady-state diffusion tests have negligible reactivity with cement matrices, are suitable for small-scale (mostly cement paste) specimens, correlate well with chlorides, and offer insights into connected porosity. However, HTO behaves differently than charged ions like chlorides in strongly charged solids (like clays), through diffusion setups require long test durations, leading to hydration artifacts, high costs and efforts, and sensitivity to concentration variations [39].

3.3 Non-steady-state bulk diffusion experiments

Bulk chloride diffusion testing involves forcing one-dimensional chloride ingress into a cement-based specimen sealed on all but one surface and immersed in a chloride-rich solution. After exposure, chloride profiles are measured to calibrate D_{nssd} (D_{app}). Initially, standardized methods such as ASTM C1556 and NT BUILD 443 employed high chloride concentrations (approximately 165 g/L NaCl or ~ 2.8 M) to accelerate chloride ingress and facilitate rapid comparative evaluation of concrete resistance [7, 8]. In contrast, more recent approaches for calibrating service-life prediction models adopt lower and more environmentally realistic chloride concentrations (typically around 0.3–1.0 M NaCl), closely matching marine splash, tidal zones, and road-deicing conditions [21]. Specifically, RILEM Technical Committee 270-CIM (2022) highlights that chloride ingress models calibrated with these realistic chloride concentrations yield significantly improved predictions of concrete durability in actual service environments compared to those obtained from highly accelerated laboratory tests [21]. This section outlines methods for testing bulk chloride diffusion at both the concrete and cement paste scales, and approaches for measuring chloride profiles in solid phases after exposure. Note that the obtained D_{nssd} is an average value of the apparent diffusion coefficient over time exposure (not an instantaneous one).

3.3.1 Concrete-scale standardized methods

The standard NT build 443 or ASTM C1556 (Table 1) was developed to measure the diffusion coefficient of concrete using a non-steady-state diffusion test. The test is destructive and time consuming (> 35 or > 90 days) because it requires the concrete to be grinded or sawn to obtain a chloride profile from titration at different depths. Concrete specimens must mature for 28 days at 20°C, be saturated with limewater, and exposed on one side to 2.8 mol/l NaCl solution (lower concentrations are now commonly employed). After 35 + days, concrete is ground in 0.5–1 mm increments to establish a chloride profile from measured

acid-soluble chloride content, excluding the first profile point from regression analysis (because of leaching and surface effects leading to peaking/plateauing behaviours near the surface [23]. More recent ISO 1920–11 and EN 12390–11 use 3 months exposure compared to 1 (to 3) month in NT Build 443, and the variation in exposure time results in differences in the obtained D_{nssd} [68]. Despite the simplifications [21, 42], Fick's second law is widely used to calibrate D_{nssd} (and C_s), As empirical parameters obtained by fitting the chloride profile with Crank's solution:

$$C(x,t) = \left(C_S - C_{background}\right) erfc\left(x/\left(4D_{nssd}t\right)^{-1/2}\right) \quad (4)$$

where C_S is the surface chloride concentration, $C_{background}$ the background concentration (initial chloride amount in the samples), x the depth, t the exposure time, and *erfc* the complementary error function.

A promising new approach for analyzing chloride profiles measured over time on concrete specimens employs the square root law of ffusion [42, 69]. In standard codes (fib), the aging exponent, a lumped parameter (Eq. 1), accounting for hydration-induced microstructure changes and binding non-linearity (RILEM TC-CIM, [22], is derived by regressing $D_{nssd}(t)$ over exposure periods (e.g., 28, 90, 365, 730 days). A key advantage of this protocol is that it avoids sawing the specimen before exposure to the salt solution, preventing early-age damage. This makes it suitable for studying chloride diffusion during cement hydration. For instance, it has been used to decouple hydration and chloride transport in slag-based mortars [70].

3.3.2 Diffusion–advection tests

There are other methods based on transient natural diffusion that also include advection effects. For example, the penetration of chloride ions can be accelerated by external water pressure or capillary suction. Chloride transport can be accelerated by applying pressure to a chloride solution-exposed face, driving advection and diffusion [71]. This method, like water permeability tests, requires a high pressure to be applied and well-sealed sample sides to prevent leakage. While theoretically sound, it is rarely used due to the need for specialized equipment and the risk of microstructure damage from high pressure.

The AASHTO T 259 ponding test (1980) [72] evaluates chloride penetration in three 75 mm slabs by exposing the top surface to 3% NaCl for 90 days while sealing the sides and drying the bottom (50% r.h.). Chloride concentration is measured in 12.7 mm slices, and results are used to estimate diffusion coefficients via Fick's second law. However, this method combines diffusion and capillary suction, potentially misrepresenting their individual effects, and its large sampling increments may introduce significant errors in diffusion coefficient calculations.

3.3.3 Miniature methods adapted for cement paste specimens

No standardized method exists for chloride bulk diffusion test on cementitious pastes, but concrete-scale tests have been scaled-down and adapted for paste specimens. Key differences between scales include casting, curing and chloride profile measurement. Cement pastes are more sensitive to inhomogeneity, bleeding, drying shrinkage and leaching (a focus of the TC 298-EBD working group 1). Homogeneity can be improved with pre-mixing of blended powders [3, 57] and two-stage mixing with water added at each stage [57, 73]. Vacuum mixing suppresses air bubbles [3, 73] and before mixing, water can be deaired [73], deionised [3] or demineralised [73]. Bleeding is a major risk at high w/c ratios, which can result in non-uniform samples, especially in terms of water distribution and microstructure. Bleeding can be mitigated by rotating samples during molding [57, 73, 74] or curing [73] and by introducing a delay in mixing (e.g., 1 h) to allow flocculation of early hydration products (reduce fluidity) [75]. Possible inhomogeneity near the casted surface can be addressed by cutting [3] or grinding [73].

The curing of cement pastes requires special care to minimize leaching. For this purpose, limewater solutions have been used to prevent the leaching of Ca^{2+} ions, but such solutions do not prevent the leaching of alkalis [76]. Another possibility is to carry out sealed curing, but there is a risk of desaturation of porosity which will impact hydration and transport. Three approaches are used to avoid a decrease in the sample internal humidity: performing sealed curing with a minimal volume of water [57], using water mixed with a powdered sacrificial sample to limit leaching of the specimen [3] or re-saturating the

sample after curing and pre-conditioning [73]. The minimal water volume approach is also supported by a recent study on the effect of curing of cement pastes on microstructure and electrical resistivity, which showed that it induces the least effect on paste properties while avoiding problems related to leaching and drying (e.g., cracking, incomplete re-saturation, etc.) [77]. The curing duration is also a variable between studies (e.g., from 28 days to 6 months). When possible, a longer curing time allows for the study of a more stabilized microstructure, resulting in a more constant diffusion coefficient over time.

Once curing is complete, a chloride-impermeable coating is applied to all surfaces of the samples except one to achieve one-dimensional diffusion. This coating is typically epoxy-based, although Jensen et al. [73] suggested the use of polyurethane. This coating can be applied on freshly cut surfaces [59, 73], or on dried surfaces [57]. If the coating process results in drying of the specimen, resaturation prior to exposure will prevent chloride penetration by advection [57, 73] as also performed at the concrete scale (e.g., ASTM C1556).

The NaCl concentration of the exposure solution varies from study to study. In most cases, the solution is prepared to simulate seawater at 3% (0.51 mol/l) NaCl [3, 59, 78] or 3.9% (0.67 mol/l) [57], but other authors also used a lower concentration of 0.115 mol/l of chloride to simulate groundwater [74]. Leaching during exposure also has an important effect on the measurement. The choice can be made to suppress the effect of leaching [73] or to include its impact by renewing regularly the exposure solution [3, 59]. The ratio of the exposed surface of the sample to the volume of the exposure solution is another important parameter for leaching; it is usually set at 50 cm^2/L, as specified in the ASTMC1556 standard [3, 66, 79]. Although this ratio has an important effect on the properties of the sample and the results, it is not always reported. The temperature is also an important parameter to report but it is not always indicated.

After exposure, chloride profiles are measured using either chemical or spectroscopic techniques (see the following section for more details). For the concrete scale, a calibration of Fick's second law of diffusion can be used to estimate D_{app} or D_{nssd}. However, analyses on cement pastes have the advantage of much higher spatial resolution (e.g., a chloride content measurement per mm), which allows better identification and understanding of the surface effects leading to peak or plateau surface behavior [23]. Additionally, controlled exposure conditions and precise measurements allow studies to be performed after much shorter exposure times, e.g. 1 day [79, 80].

Similarly, while the square root law for chloride diffusion was initially developed for analysing long-term concrete exposure [69, 81, 82], its application to cement paste samples has enhanced understanding of chloride ingress behavior [3, 42, 80, 84–86]. For example, Wilson et al. studied transport and binding properties of various blended cement systems exposed to seawater-like chloride concentrations, showing that penetration is primarily diffusion-driven, with little effect of the very different binding behavior, i.e., chloride penetration obeys the square root law with an offset to account for microstructural changes that occurred prior to the first measurement [3, 50].

Moreover, the penetration depth at a reference chloride content divided by the square root of time ($X_{Cr}/\sqrt{t}$) turns out to be a good indicator of the resistance against bulk chloride diffusion and correlates very well with D_{app} [3, 83]. Further research is needed to strengthen the use of square root law to model chloride diffusion, but this can be very promising as measurements could be simplified by focusing only on penetration depth rather than full profiles.

Fitting chloride profiles with Crank's solution to Fick's law provided apparent diffusion coefficients (D_{nssd}) and surface chloride concentrations (C_s), summarized in Table 4. Across all systems, the differences between SEM–EDS and grinding titration (GT) methods remain within ASTM C1556 limits ($\leq$39.8% for D_{nssd}, $\leq$37.2% for C_s), indicating acceptable inter-method variability. The observed differences (d_{2s}), while sometimes high (e.g., 32% for D_{nssd}), are typical due to the sensitivity of the fitting equation to slight profile variations. SEM–EDS consistently yields slightly higher values than grinding titration and is better suited for short-term exposure measurements due to its superior spatial resolution.

3.3.4 Methodology for chloride profile measurements in the solid phases

Measuring chloride profiles after bulk diffusion tests can be done by different methods based on five principles: chemistry-based techniques, X-ray spectroscopy,

Table 4 Effect of SCMs (GGBFS = Slag, Fly Ash = FA, Calcined Clay = CC) on Fick's 2nd solution fit parameters D_{nssd} and C_s for chloride concentration profiles measured by SEM–EDS and grinding titration (GT) after 100 days of exposure in 0.5 M NaCl. The difference between the SEM–EDS and GT methods is indicated as d2s

Paste mix (w/b = 0.4)	$D_{nssd\ EDS}$, 10^{-12} m^2/s	$D_{nssd\ GT}$, 10^{-12} m^2/s	$d_{2s,}$ %	C_{sEDS}, wt%	$C_{s\ GT}$, wt%	$d_{2s,}$ %
100%OPC	11.36	8.23	32.0	1.78	1.80	1.1
100%PLC (30% CaCO3)	11.81	14.15	18.0	0.53	0.50	5.8
70%PLC + 30%GGBFS	1.12	0.90	21.8%	1.65	1.84	10.9
70%PLC + 30%FA	3.76	3.70	1.6%	3.21	2.25	35.2
70%PLC + 30%CC	0.42			1.88		

X-ray absorption, plasma spectroscopy and mass spectroscopy. These methods are generally easier to apply to cement paste samples, but they can also be used for concrete by either identifying its individual components or assuming that only the paste fraction contributes to chlorides binding. The methods are briefly described here in the context of obtaining chloride profiles, but further review of each method itself can be found in a previous review on measuring chloride binding in cementitious materials prepared by RILEM TC 298-EBD [86].

In concrete, chlorine is mainly present in the form of chloride, either dissolved in the pore solution or bound in salts and hydrated phases. However, due to their physical measurement principles, many analytical techniques detect elemental chlorine. For simplicity, the term chloride is used throughout this section, even when referring to measurements based on chlorine.

3.3.4.1 Chemistry-based techniques Currently, the most used technique is the chemical titration of ground powder (ASTM C1152, ASTM C1218, AASHTO T 260–21, NT Build 208, [11–13]. Sample is sliced into thin layers, ground into powder, and chlorides extracted using nitric acid or water. Chloride concentration is then measured by potentiometric or Volhard titration method [86].

Acid dissolution measures total chloride, while water extracts free and some bound chlorides [87]. Bonnet et al. [88] quantified the source of uncertainties for total chloride profiles measurements by considering human, instrument and protocol errors. The grinding/titration method, though common, has limitations: labor-intensive, error prone [89], low spatial resolution (1–2 mm) and variable accuracy depending on pH [90]. It works best for cement paste but requires large samples for mortar and concrete due to chloride dilution and lower spatial resolution.

Colorimetric measurement using $AgNO_3$ spray [91] on a cross-sectioned specimen forms a silver-gray AgCl precipitate in chloride-rich regions [92], allowing visualisation of the chloride penetration front and determination of the characteristic concentration C_d (the chloride concentration corresponding to the colour change at penetration depth x_d). It is fast and simple but depends on pore solution alkalinity [93], C_d varying between 0.07M and 0.7M (free chloride) in different mixes [93], limiting its reliability across blended binders [94]. If Cd and surface chloride are known, diffusion coefficient can be estimated [3, 7]. These C_d values should be discussed in the future to better assess the value of D_{app} in the case of concrete with SCM. Moreover, distinguishing color changes is difficult, especially in dark or low-penetration samples. Modified methods using K_2CrO_4 or fluorescein [95] improve visibility. Downscaling the study to cement paste mitigates heterogeneity issues due to aggregates [96].

Due to the limitations of the titration of chloride and the colorimetric techniques, alternative techniques were developed. Some of these methods rely on the excitation or ionization of atoms using an external energy source, causing them to emit characteristic X-rays as they return to a lower energy state. Different energy sources can be used: X-ray beam for µXRF [97], electron beam for Energy Dispersive X-ray Spectroscopy (EDS) or Electron Probe MicroAnalyser (EPMA) [98–101] and particle beam (PIXE) [102]. These techniques allow characterising chemically the sample and creating maps of the chemical composition, which can be divided into

slices and the mean chloride content of every slice is used to obtain the profile. A more detailed review of the methods can be found in the previous TC 298-EBD publication [86].

Depending on the source of energy, the resolution, and the limit of detection of chloride content varies. These values are given in the Table 5. In most cases, the spatial resolution is improved compared to the titration so that the profile obtained is more precise thanks to the smaller sample volume under investigation.

Another advantage of these techniques compared to titration is the ability to map the chloride concentration, so that only the cement paste is studied in mortar samples after excluding aggregate volumes from the measurement data using criteria on calcium and silica contents [89, 100].

In the case of EDS and EPMA, the sample needs to be cut, impregnated in epoxy, polished and coated with carbon to evacuate charge. These manipulations are risky because it can be a source of contamination of the sample with chloride, displacement of chloride or carbonation products. To prevent these risks, ethanol is used as a lubricant for both cutting and polishing [99] but it can also be a dry cutting [92]. Bernard and Wilson [103] proposed a simplified protocol using variable pressure SEM–EDS to quantify chloride ingress without complex calibration or extensive sample treatment. The procedure measures chloride profiles at various depths across ~ $200 \times 900\ \mu m^2$ areas, large enough to average local variations and minimize surface preparation effects. Depth intervals ranged from 300 µm to 2.5 mm, enabling fine resolution near the surface and efficient analysis for deeper ingress. The measured concentration was assigned to the central depth of each area, with image analysis used to determine the exposed surface. Varying the chamber pressure between 0.1 and 10 Pa showed no significant effect on quantification. A strong correlation ($R^2 = 0.993$) between SEM–EDS at 0.1 Pa and grinding titration confirms the method's quantitative validity. Differences between methods were under 10%, indicating good agreement. Chloride profiles measured on OPC and LC3 blends specimens after 36 days matched ASTM C1556 criteria for repeatability, validating the proposed SEM–EDS protocol.

For the µXRF measurement, no coating is necessary, and the polishing is less sensitive thanks to the greater depth of penetration of X-ray in the sample. Finally, the PIXE does not require any sample preparation. Calibration of spectroscopy methods can be useful, but not necessary [3].

Laser-Induced Breakdown Spectroscopy (LIBS) is another technique for estimating chloride content in cementitious materials [104]. In this method, a high-energy laser ablates the sample surface, generating a plasma that emits light analyzed spectroscopically to determine elemental composition. LIBS is an established method for chloride analysis in concrete, as outlined DGZfP bulletin B14 [105]. Laboratory studies have demonstrated its sensitivity, with detection limits for chloride in cement paste samples averaging approximately 0.09 wt.% [106]. For accurate quantification, however, matrix-matched calibration samples are required [107].

Sample preparation for LIBS is minimal, requiring only the splitting of concrete cores, and measurements can be performed directly on rough surfaces [105]. The technique enables spatially resolved measurements, preserving critical localized information

Table 5 Comparison of the chemical titration of ground powder with other Cl profile measurement methods

Technique	Detection limit (wt.% cement)	Spatial resolution	Notes
Chemical titration	< 0.01 [117]	1–2 mm [7]	Standard, widely used
Colorimetry	/	/	Less detailed info
EPMA	0.01 [99]	0.5 µm [100]	High spatial resolution
EDS	0.1–0.2 [118]	37 µm [118]	Suitable for fine profiling [103]; validated SEM–EDS protocol*
µXRF	0.1 [89]	50 µm [89]	Moderate resolution
LIBS	0.09 [106]	100 µm [119]	Laser-based technique
LA-ICP-MS	0.12 [120]	300–400 µm [120]	Sensitive but coarser resolution
TXM	/	8.8 µm [121]	X-ray microscopy method

*Variable pressure SEM–EDS with minimal sample prep and no complex calibration [103]:

about chloride distribution such as in cracks, which would otherwise be lost through sample homogenization. The spatial and local resolution of LIBS depends on the specific system used and can achieve scales below 100 µm or even finer. Additionally, LIBS facilitates simultaneous multi-element analysis, enabling the selective analysis of the binder matrix in concrete samples by identification of individual concrete components [108–110], thereby providing a direct correlation between chloride content and the binder phase. Its reliability for chloride analysis is further supported by good agreement with acid-soluble methods [111]. Moreover, the availability of remote and portable LIBS systems expands its utility for rapid field measurements [112].

A key advantage of LIBS over many other analytical methods is its ability to detect light elements, including hydrogen, providing a broader element analysis capability. Although measurements can be performed under atmospheric conditions, signal quality can be enhanced by introducing an inert gas around the plasma [104], dual pulse configuration [113], electric sparks [114], or microwave coupling [115]. Despite its considerable potential, LIBS remains underutilized within the cement community, with its commercial application largely confined to a few specialized laboratories, primarily in Germany and Switzerland.

LA-ICP also utilizes the plasma state of the sample for chemical characterisation and can therefore be used to measure spatially resolved composition [74]. The sample undergoes laser ablation, transported in argon, and transformed into plasma by induction. The ions created are chemically segregated by a mass spectroscopy according to their mass to charge ratio. Measurements can be performed directly on solid surfaces, but accurate quantification requires careful system calibration. Finally, it has a particularly good resolution and limit of detection (see Table 5).

Transmission X-ray microscopy (TXM) technique uses the difference in absorption of X-ray between a cement paste with a high concentration of ions and another one with a low concentration of ions. Because of the weak ability of chlorides to absorb X-ray, they are replaced for this test by iodides that are of comparable size and more absorbent. The diffusion test is made with a solution of KI and then X-rays are transmitted through the sample. The profile of iodide is then obtained with the profile of absorption of the sample. It is possible to make a calibration of the test to obtain quantitative values. The main drawback of this technique is that it does not use chloride but iodide that has a different size, ionic mobility and binding ability so the diffusion coefficient varies slightly compared to that of chloride [116]. The possible differences in behavior, especially for liquid/solid interaction, makes this method not adapted to diffusion with binding. Mortar or concrete samples make the measurement more complex because iodide shows nonuniform penetration when the solution reaches large features like aggregates.

3.3.4.2 Comparison of the methods with potentiometric titration In addition to the well-established approach of sample grinding followed by potentiometric titration, several alternative analytical techniques are available for the quantification of chloride in concrete. These methods offer various advantages, notably in terms of sample preparation: most can be applied directly to freshly split or polished core surfaces, eliminating the need for extensive sample preparation.

Surface scanning techniques, in particular, provide improved spatial resolution, enabling a more accurate assessment of chloride ingress, especially in the presence of cracks. Moreover, they facilitate the selective analysis of distinct concrete components, allowing for a direct correlation between chloride content and the binder phase.

All methods considered offer detection limits sufficient for identifying critical chloride concentrations (0.2–0.5 wt.% per binder), as summarized in Table 5. However, accurate quantification often requires the use of matrix-matched calibration standards. In addition, some of these techniques support in-situ measurements with portable or remote-operable devices.

- Depth intervals: 300 µm to 2.5 mm
- Validated repeatability per ASTM C1556 for OPC and SCM blended cement pastes

4 Migration tests

Several types of rapid chloride penetration tests have been developed over the last decades. Common to all is that a concrete sample is placed adjacent to a chloride solution on the one side and a chloride-free

solution on the other. A potential difference is then applied to drive chloride ions through the concrete. A chronological review of reported test methods is first presented in this section, followed by specific descriptions of current steady-state and non-steady-state migration methods for concrete and cement pastes.

4.1 Historical development of migration methods

The first type of rapid test is represented by the AASHTO T277 test [122], developed by Whiting [123], in which the total charge passed through a sample during a six-hour period under a 60 V potential difference is measured, and the value is used as a chloride permeability index. The second type of test reported is developed by Dhir et al. [124], who related the measured steady state chloride flux under a 10 V potential difference empirically to the chloride diffusion D of the concrete. The D values from Fick's first law exceeded conventional natural diffusion coefficients, making it an index of chloride diffusion rather than a true D.

The third type of test is represented by the developments of Tang and Nilsson [125], further standardized as NT-Build 492, in which the depth of chloride penetration under a 30 V potential after 8 h is measured. In their proposed method the authors established a relationship between the penetration depth of chloride ions and a chloride diffusion coefficient D_{nssm}. based on the measured c_d, the chloride concentration at which the colour changes when a colorimetric method is used to measure the penetration depth x_d.

In NT Build 492 [16] and NF XP P18-462 [17] the diffusion coefficient calculated through this method is defined as D_{nssm}, reflecting that this value is calculated through a non-steady state migration transport process. Even in the case of the method proposed by Dhir et al. [124], although Fick's first law of diffusion was used for calculation of the index of chloride diffusion, the test set-up was not following a steady state transport regime. Andrade [126] presented a theoretical steady-state migration test method suggestion, which was further experimentally tested and presented in (Andrade et al., 1994) [127] and modified to become the standard NF XP P18-461 (details are provided in Sect. 4.2).

Tang [128] also suggested a steady-state method which was adapted from the method by Whiting [123]. Andrade [126] proposed a steady-state migration test method, later further experimentally validated [2, 129].

As stated in [128] the greatest difference between the steady-state migration and non-steady-state migration is that in the former the chloride ions must pass through the specimen and the flow rate must be measured until steady-state flow is obtained. Another difference is the destructive aspect of the non-steady state migration coefficient. Indeed, the specimen could be used after the test for other measurements as done by Djerbi el al. [130, 131] to evaluate the influence of damage on chloride ingress. Given the longer time duration of the method, durable anodes should be used such as platinum to maintain a clean anolyte solution, while evaporation in anolyte should be prevented. Given the experimental duration, thinner discs are suggested (30 mm) than in the case of non-steady-state migration (50 mm). A lower applied potential (24 V) compared to non-steady state migration (30 V) is also recommended to keep the electrical field to 600 V/m. A high concentration of chloride in anolyte should be avoided as the produced hydration phases might cause pore blockage and consequently decreased flow. A solution of 3% NaCl in 0.1 M K/Na (OH) solution is suggested. To prevent production of chlorine gas the pH value in anolyte should be kept to more than 12. Therefore, a 0.3 M K/Na (OH) solution and frequent control of the pH in anolyte are important [132]. However, controlling the chloride concentration in the downstream cell is challenging due to limitations in measurement accuracy and potential chemical reactions at the anode. Therefore, further improvements of the method were suggested by Truc et al. [133], in which instead of controlling the concentration in the down-stream cell, a control for upstream cell was suggested. Further, Castellote et al. [134], presented an update in the method in which monitoring of the conductivity of anolyte chamber was suggested instead of concentration measurements. Their work is an attempt to also account for chloride binding by means of calculating the time-lag taken by the chlorides to appear in the downstream or anolyte chamber.

It is, however, important to not underestimate the effect of migration on pore solution characteristics of the cementitious sample through the migration test. As presented by Cherif et al. [135], the ionic concentrations change in the sample during a migration test.

Decomposition of portlandite, calcium release and the decrease of Na^+ and K^+ in the sample pore solution are important aspects not usually considered in literature. Moreover, as presented by Hemstad et al. [136], the capacity of the paste to bind chlorides is a complex function which can be affected by phase assemblage and chloride concentration as a function of depth, pH and leaching. These outcomes infer that the calculation of bound chlorides through a migration test might have inaccuracies assigned to it.

4.2 Steady-state migration experiments

NT Build 355 and NF XP P18-461 background is introduced in the previous section. Its main drawbacks are discussed in following section.

To estimate D from migration measurements in concrete, three key factors are considered: *1*) Experimental data collection—monitoring chloride flux (J) over time while applying a suitable potential difference (ΔE) to drive migration *vs* minimizing the Joule effect. 2) Solving the Nernst-Planck equation—relating flux to D_{ssm}, simplified as (see assumptions below):

$$D_{ssm} = JRTL/\left(zFC_{cl}\Delta E\right) \tag{5}$$

or alternatively to 2, 3) Using the Nernst-Einstein equation—linking flux to total current intensity (i) and the transference number (t_j-) of migrating anions, yielding: $J = (i\ t_j)\forall(n\ F)$. By calculating the transference number (t_j) from the experimental data and substituting it into the simplified equation to obtain D_{ssm}:

$$D_{ssm} = RTit_{cl}/\left(nF^2\Delta EAC_{cl}LZ\right) \tag{6}$$

where L is the specimen thickness. The framework for calculating D_{ssm} (NT Build 355 introduced 1997), considering steady-state flow, potential difference, and ionic strength in concrete pore solutions is based on following assumptions. No advection, diffusion is negligible at ≥ 10V, chloride concentration is constant upstream, and the electric field decays linearly across the specimen. Ionic mobility is higher in solution than in the sample (L is the transport distance). The mathematical equations from Andrade and Tang [126, 128, 129] were similar with a minor difference being Andrade's [126] inclusion of chloride ion activity, which Tang excluded due to dominance of strong external electrical current.

4.2.1 *Concrete-scale methods*

The ASTM C1202 'Coulomb test' measures charge passed (based on Nernst-Planck and flux related to transference number, see previous section) as an index of chloride resistance but cannot directly determine D due to the involvement of all ions [137]. However, using almost the same setup, a steady-state diffusion coefficient can be theoretically calculated, as outlined in NT Build 355 [16] (Table 1). The chloride migration coefficient can be determined by measuring the electrical current over time and analyzing it with the Extended Nernst-Planck model (Samson 2003) [138], while other species' migration coefficients are computed based on their diffusion coefficient ratios relative to chloride at infinite dilution.

However, in the experimental setup chloride ions may convert to chlorine gas in the downstream cell, which is difficult to control and quantify. Additionally, the electrical potential between electrodes, rather than across the specimen, is used in calculations, ignoring the potential drop at the specimen surface. The model also assumes a single species theory, neglecting interactions with other ions. To address the single specie limitation in obtaining D_{ssm}, Zhang et al. [139] introduced a correction factor (β_0) dependent on (NaCl) concentration and temperature. Zhang et al. [140] developed an electrochemical approach linking observed migration rates to D_{eff}, while NF XP P18-461 refined Andrade's methods, using potentiometric titration to demonstrate equivalence between $D_{eff\ (migration)}$ and D_{ssm}. Castellote et al. [134] presented a faster migration test by monitoring downstream (anolyte) conductivity, though it excluded D_{ssm} determination. Truc et al. [133, 141] proposed strategies to address limitations in steady-state methods, focusing on pore structures and assuming the upstream flux (being constant from the test start and independent of chloride binding). Together, these works advanced rapid chloride diffusion assessment in concrete. Neglecting electroneutrality in NT Build 355 underestimates D; an order of magnitude compared with a Friedmann's steady state migration method based on current measurement and Nernst-Planck (with electroneutrality) analytical model (Friedmann, 2004) [142]. KrabbenhØft et al. [143] used coupled Nernst-Planck-Poisson model for migration tests and found effective diffusivity differences of 50–100% compared to single-species models

like NT Build 492 and NT Build 355. KrabbenhØft suggested adjusting the NaCl/NaOH ratio in cells to improve results with simplified models.

Finally, the unclear behavior of chloride ion binding under an electric field may introduce systematic errors, highlighting the need for further research across different current densities.

4.2.2 *Miniature methods for cement pastes*

While most studies have been carried out on concrete specimens, researchers have also developed test setups to perform migration tests on paste-scale specimens, sometimes referred to as "mini-migration tests" (2004) [75, 144, 145] (Fig. 4). The parameters and differences between these methods are presented in Table 6. Note that less experimental details have been reported by Hu et al. [145] which limits the comparison with the other reported methods. They used kaolinitic clays mixed with Singapore's low-grade marine clays (16–20% kaolinite and illite and quartz as major phases). When used in LC^3 systems, these clays reduce 28-day strength by 25% compared to OPC, but promote CO_3-AFm formation, improve chloride resistance by an order

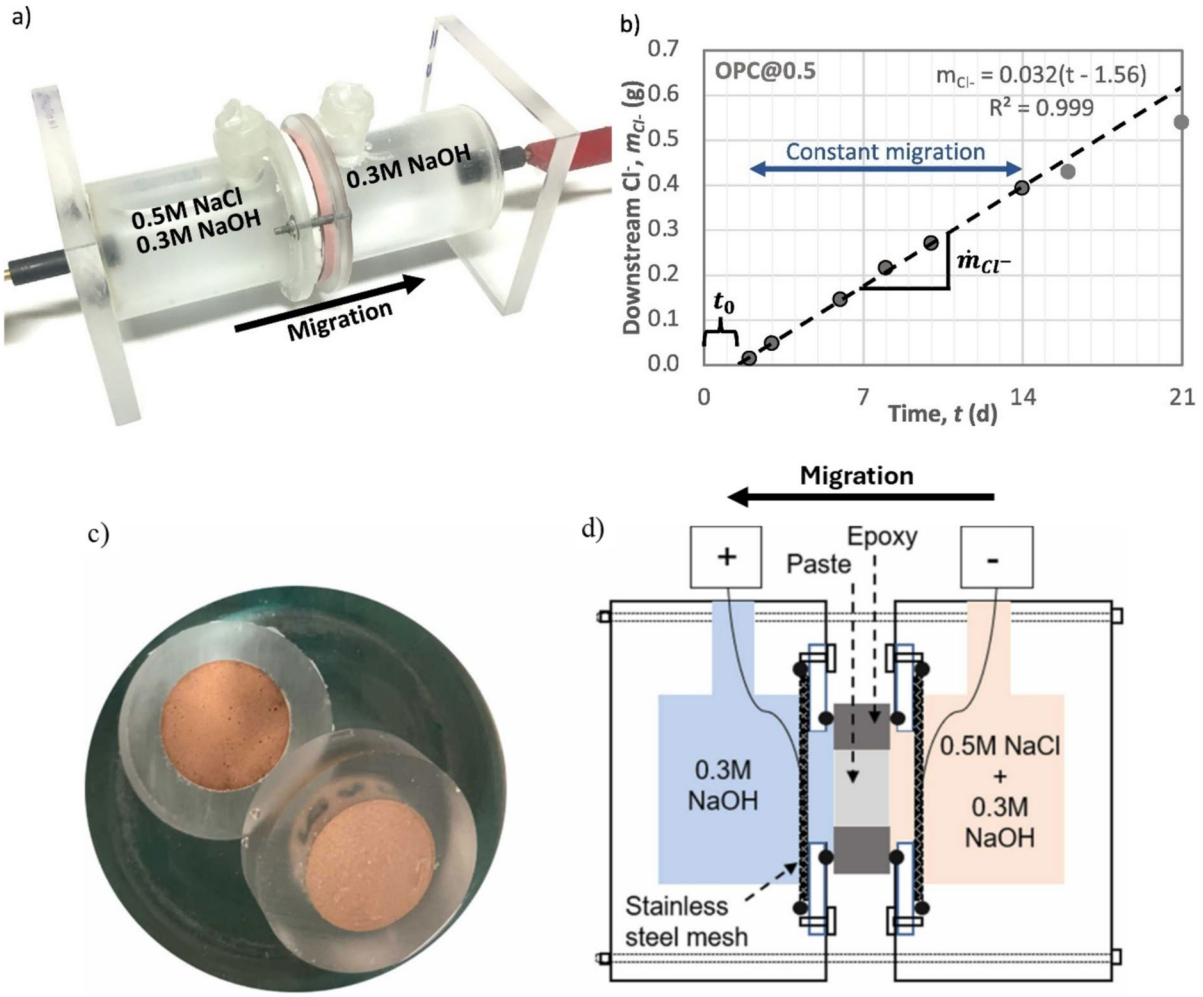

Fig. 4 Wilson et al. [75]: a) A mini-migration setup drives chlorides through a 33 mm × 10 mm cement paste disk. b) For OPC (w/b = 0.5), $AgNO_3$ titration of downstream samples shows steady chloride migration after breakthrough (t_0), lasting until reservoir concentrations shift (t > 14 days). Hu et al. [145]: c) Cement paste samples flat cylinders with epoxy covering the lateral sides; d) mini-migration set-up scheme

Table 6 Comparison of the miniature steady state migration methods for cement pastes

Method	NT Build 355	Ait Mokhtar et al. [144]	Wilson et al. [75]	Hu et al. [145]
Curing	Water at 20 ± 2 °C	Downstream solution	Sacrificial solution	Sealed curing
Curing time	91 days	28 days	28 days	28 days
Pre-saturation	Yes	No	Yes	Yes
Polishing	No	No	Yes	Yes
Core sampling	Yes	Yes	No	No
Sample dimensions	95-100 mm diameter and 50 mm thick	63 mm diameter & 10 mm thickness	33 mm diameter & 10 mm thickness	
Voltage	12 V	300 V/m = 3 V	5; 12 V	5; 12 V
Reservoirs sizes	Measured before test	1 L downstream, 2 L upstream	125 mL each reservoir	113 mL
Downstream solution	300 mM NaOH	25 mM NaOH + 83 mM KOH	300 mM NaOH	330 mM NaOH
Upstream solution	860 mM NaCl	Downstream + 500 mM NaCl	Downstream + 500 mM NaCl	Downstream + 500 mM NaCl
Solution renewal	To maintain the concentration in the upstream reservoir	10–15 h	None	
Test duration	> 7 days	14 days	2–3 weeks	
Measured quantity	Voltage drop and downstream Cl content	Current & downstream Cl content	Downstream Cl content	Downstream Cl content
Frequency of measurement	At least each days	N/A	2–4 days	1–3 h
SCM effects	$\downarrow D_{ssm}$ mostly due to refinement of pore structure by SCM (Fig. 5); linear correlation with bulk conductivity (not normalised)			

of magnitude (Fig. 5a), and refine pore structure despite increased porosity.

The proposed methods are down-scaled adaptations of the AASHTO T277 test setup [122], developed by Whiting [123]. The current and/or chloride concentration are measured over time and a diffusion coefficient is calculated based on the approach of Andrade [129]. As with the diffusion tests, when scaling down to the cement paste scale, special attention must be paid to possible problems with sample preparation, bleeding, drying, leaching and more.

Wilson et al. [75] observed a strong correlation between D_{ssm} and bulk conductivity σ_b (Fig. 5b) for a wide range of SCM (CC, LL, GGBFS, FA, glass powder) and w/b ratios, supporting that both tests can characterize the effective chloride ingress, with D_{ssm} being useful in transport models. They thus conclude that bulk conductivity is a good indicator for chloride ingress resistance and that it should not be normalized by the pore solution conductivity due to the impact of the pore solution on diffusion. In addition, the use of the mini-migration setup allows in-depth analysis and understanding of migration-related phenomena, as complementary experimental techniques can be used to examine the exact same cement paste samples before, during and after mini-migration, in terms of microstructure (e.g. with mercury intrusion porosimetry), phase composition and chemically bound chlorides (with XRF and XRD), elemental and phase profiles (with SEM–EDS), together with the composition and conductivity of the pore solution. Such coupled analyses allowed to distinguish the mode of action of different SCM on chloride diffusivity (i.e. pore network properties vs. pore solution conductivity) [146].

4.3 Non-steady-state migration experiments

4.3.1 Concrete-scale standardized methods

The NT BUILD 492 method [16] is a widely used rapid non-steady-state migration test for assessing chloride penetration resistance in concrete, mortar and cement-based repair materials [147]. This method relies on chloride ion migration under an external

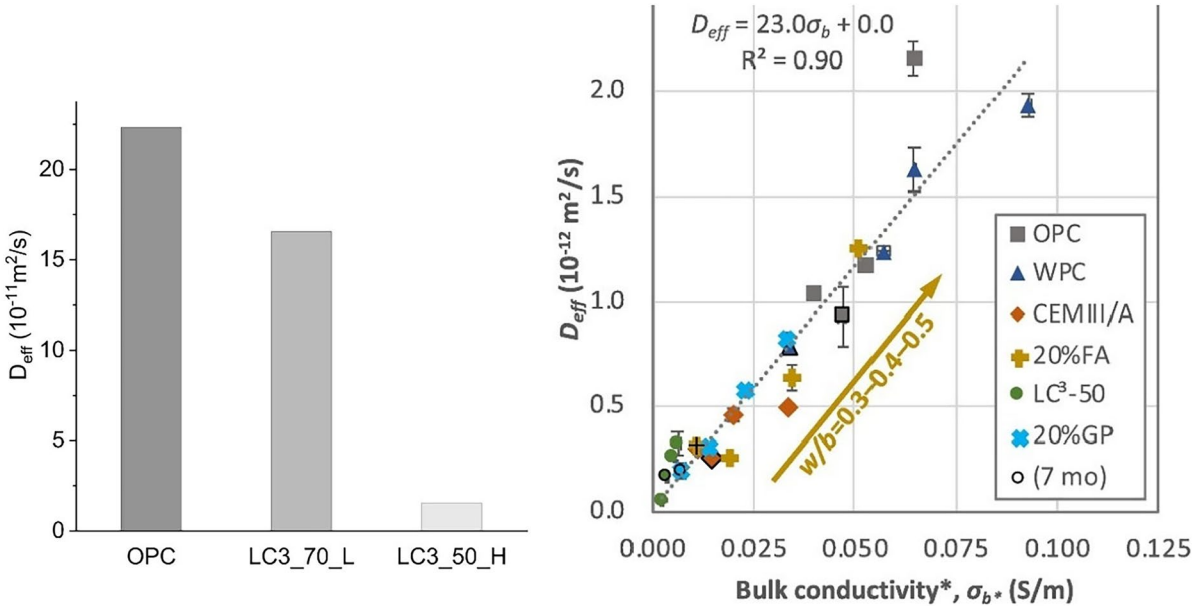

Fig. 5 **a** Hu et al. [156] results of Dssm (=Deff; LC3_70_L has 71% OPC +18 % low grade 3 mixed calcined clay; and LC3_50_H has 53% OPC + 15 % metakaolin rich and 15% low 4 grade mixed calcined clay). **b** Wilson et al. [78] linear correlation between Dssm (=Deff) and 5 bulk conductivity taken as the average between 28-day and 91-day results to consider 6 microstructure changes occurring during the mini-migration test

electrical field, using a potential difference and a colorimetric indicator (0.1 M AgNO3 spray). It provides quantitative data, including chloride penetration depth and diffusion coefficient, with test durations ranging from 24 h for ordinary concrete to 96 h for high performance concrete [148]. In NT BUILD 492, specimens (100 mm diameter, 50 ± 2 mm thick) are sliced from cast cylinders or drilled cores with a minimum length of 100 mm. NT Build 492 (the basis for EN 12390–18 and XP P 18–462) involves specimen pre-saturation pre-treatment (under vacuum and with a $Ca(OH)_2$ solution), using a 10% NaCl upstream solution. In contrast, EN 12390–18 does not use vacuum pre-saturation and samples are cured in water without $Ca(OH)_2$, but the method uses an upstream alkaline solution, i.e., 5% NaCl in 0.3 M NaOH.

A DC potential of 30 V is applied, adjustable between 10 to 60 V to limit specimen power consumption to less than 2 W. After the test, the specimen is split and chloride ion penetration depth is determined using a colorimetric method [76]. Chloride penetration depth is measured every 10 mm on each split piece, yielding 5 to 7 valid readings per specimen. To ensure safety and minimize contamination, $AgNO_3$ spraying should be performed in an enclosed space. The chloride diffusion coefficient (D_{nssm}) is calculated as:

$$D_{nssm} = \frac{RTL}{zF\Delta E}\frac{x_d - \alpha\sqrt{x_d}}{t} \tag{7}$$

where x_d is the average value of the penetration depths, t is the test duration. α is a laboratory constant (Eq. 8):

$$\alpha = \frac{2}{\sqrt{a}} erf^{-1}\left(1 - \frac{2C_d}{C_0}\right) \tag{8}$$

The NT BUILD 492 offers good precision, with a repeatability COV of 5–9% and a reproducibility COV of 12–24% (13% for Portland cement or silica fume concrete, and 24% for slag cement concrete) [149]. It is a simple, rapid method with straightforward calculations, producing results comparable to the longer NT BUILD 433 tests [149]. However, the theoretical model has notable oversimplifications [150]. It assumes independent chloride ion movement, neglecting interactions with other ions in the pore solution [150]. The method also presumes a constant electrical field and disregards chemical

reactions with the hydrated paste [138, 147]. Moreover, the accuracy of colorimetric method is questionable, as the *Cd* value is affected by SCM due to their effect on pH. This point needs more introspection in the future.

Tang et al., noted significant depth measurement errors at shallow depths, though errors at depths over 10 mm can be reduced to a few percent [151]. To minimize specimen heating, the increase in applied voltage should be controlled, and the volume of the salt solution increased [152]. Excessive potential difference can lead to overheating, altering results, and damaging concrete specimens [153].

As shown by Hemstad et al. [136], chloride binding capacity depends on phase assemblage, concentration, depth, pH and leaching. The unclear behavior of chloride ion binding under an electric field may thus introduce systematic errors. Additionally, the kinetics of binding, both during and after the application of the voltage, warrant investigation. Specifically, delays in conducting profile tests could influence ongoing binding reactions, particularly if equilibrium has not yet been reached. Another major drawback of many electrically accelerated methods is their reliance on single-species theory, which neglects the influence of other ions. While coupling the Nernst-Planck and Poisson equations improves theoretical accuracy, it remains too complex for practical engineering use. Friedmann's analytical solution [142], which incorporates the Nernst-Planck model and electroneutrality, shows promise, but further efforts are needed to make the experiment more practical and applicable to non-steady-state conditions.

Finally, one should keep in mind that in durability prediction models, using input D parameters obtained by migration methods is considered as an empirical approach [52, 154] where D_{nssm} should always incorporate a calibration factor to account for the correlation with $D_{\mathrm{app}}(t)$ [68, 155].

4.3.2 *Miniature D_{nssm} methods for the cement paste scale*

Huang et al. [156, 157] modified the NT BUILD 492 to evaluate chloride migration in pastes blended with fly ash, slag and limestone. The primary adjustment for paste was reducing specimen size to prevent cracking, using rubber cylinder moulds with a 50 ± 2 mm diameter (half that of concrete samples) and 110 mm length. Pastes were sealed cured for 1 day, demoulded, and water cured until the target ages (e.g. 28, 90, 180 days). For RCMT, two 50 ± 2 mm thick samples were cut from each specimen, and a preset voltage of 40 V was applied to determine the initial current. Penetration depth was measured at ~ 5 mm steps after the white silver chloride precipitation was visible on split surfaces, following NT BUILD 492 procedures. Similarly, Ranger and Hasholt (2023) [158] used smaller samples (22 mm diameter) for chloride migration tests, measuring only two depths per specimen to determine the penetration depth (Table 7). The calculation of D_{nssm} for pastes followed the same equations used for concrete samples. Table 7 compares the key setup differences between standard concrete tests and these customized paste methods. Practical challenges include potential sample breakage or accelerated dissolution at the interface between clamped and unclamped regions after testing, especially if the applied current is too high. This can complicate the accurate measurement of penetration depth.

The miniature methods at paste scale effectively quantify the influence of SCM on the chloride migration in cement-based materials. Huang et al. (2022a) [157] demonstrated that the major cause of changes in migration coefficient of blended pastes is the refinement of pore structure by SCM. This refinement can be assessed by the electrical conductivity properties of cement-based materials [159]. Ranger and Hasholt [158] found that the D_{nssm} of paste correlated with the reactivity of the SCM (Fig. 6), and the inverse of formation factor ($1/F$, where formation factor F is the sample conductivity normalized by the conductivity of the bulk pore solution). Moreover, they found a clear correlation between paste and concrete properties, regardless of binder type, though aggregates affect D_{nssm} and bulk conductivity differently, altering their proportionality coefficient. Thus, transport properties of concrete can be compared using paste data, if aggregate type, volume, and grading are consistent.

Huang et al. [156] found a strong linear correlation ($R^2 = 0.98$) between D_{nssm} and $1/F$ (inverse formation factor, Fig. 7), outperforming conductivity-based correlation ($R^2 = 0.96$). Since pore solution conductivity is affected by saturation, chloride migration is primarily governed by pore structure. The regression slope (2.037×10^{-9} m^2/s) aligns with chloride migration in dilute solution, confirming that $1/F$ reliably predicts

Table 7 The difference of D_{nssm} procedures between concrete samples and the adapted paste tests. The last row summarizes the effect of SCM on the test results

Procedures/setup	NT BUILD 492 [16]	Huang et al. 2022 [156, 157]	Ranger and Hasholt, 2023 [158]
Curing	No specific requirement	Water curing	Sealed curing
Curing Time	No specific requirement	28 d, 90 d, 180 d	28 d
Pre-conditioning	Yes	No	Yes
Samples length	50 ± 2 mm	50 ± 2 mm	50 mm
Sample diameter	100 mm	50 mm	22 mm
No. of profile depth datapoints per specimen	7	4–5	2
Voltage (for $I_{initial}$)	30 V	40 V	30 V
Upstream solution (Catholyte vol.)	10 w. % NaCl in tap water	10 w.% NaCl (12 L)	10 w. % NaCl (3.5 L)
Downstream solution (Anolyte vol.)	0.3 M NaOH in distilled or de-ionised water	0.3 M NaOH (300 mL)	0.3 M NaOH (20 mL)
Temperature	Maintain in the range of 20–25 °C	19–20 °C	–
Test duration	6–96 h (depends on sample)	24 h	24 h
SCM effects	$\downarrow D_{nssm}$ mostly due to refinement of pore structure by SCM (Figs. 6 & 7); linear correlation with normalised bulk conductivity		

chloride migration in cement pastes, accounting for SCMs and hydration effects.

5 Final remarks and perspectives

5.1 Overall comparison of methods

The model simplifications (with the corrections presented in Sect. 1) provide different definitions of D used in the different test methods. They are now integrated in an overview of pros and cons (Table 8), which forms a basis to summarize implications of the SCM on relevant model simplifications both from measuring and predicting point of view.

Bulk diffusion test (NT Build 492) currently appears to be the most suitable method for non-steady-state migration testing. In accelerated tests, correlations with diffusion tests are required, to use relevant D in model predictions. Moreover, complicated coupled processes like binding (kinetics) in accelerated tests (e.g. under and after electric fields) complicate establishing such correlations. Single-species theories neglect ion interactions, and while advanced models improve accuracy, they require refinements for practical use.

Table 9 provides a concise comparison of diffusion and migration methods for measuring chloride transport in cementitious materials, highlighting suitability for paste applications. It evaluates steady-state and non-steady-state approaches in both diffusion and migration tests, emphasizing accuracy, field relevance, and practical challenges. Diffusion and migration methods each have strengths and limitations for measuring chloride transport in paste samples. Non-steady-state diffusion (D_{nssd}) provides the most realistic and comprehensive results but requires long test durations and precise equilibrium data, while migration methods offer faster results but rely on simplifying assumptions, making them less field-relevant. Sample preparation plays a critical role in ensuring the reproducibility and reliability of chloride transport measurements in cement pastes. As outlined in Table 10, standardized guidelines—including vacuum mixing, water quality control, bleeding mitigation, and proper curing protocols—are recommended across all test types to produce uniform and representative specimens. These steps are essential to reduce artifacts such as microstructural heterogeneity or

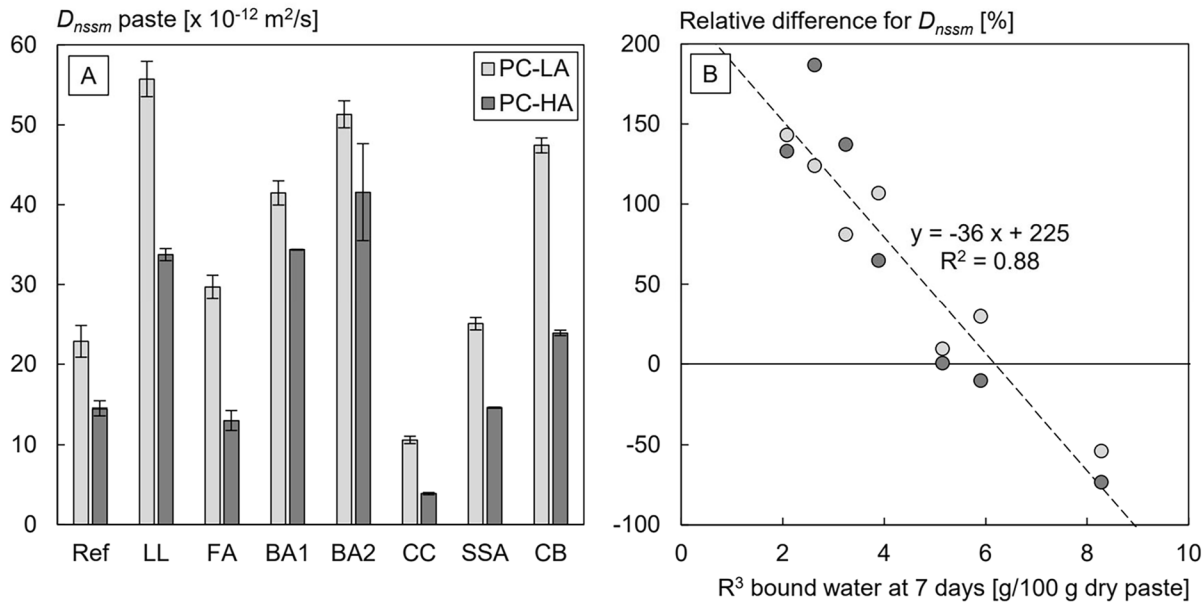

Fig. 6 Ranger and Hasholt [158]: **a** Results of miniature D_{nssm} from blended cement pastes (low and high alkali PC (PC-LA and PC-HA) blended with LL-limestone; FA-Fly Ash, BA-Biomass Ash, SSA-Sludge Ash, CB-crushed Bricks) hydrated for 28 days. **b** Effect of SCMs on Dnssm (% of the OPC value) correlated with the SCM reactivity (R^3 bound water test)

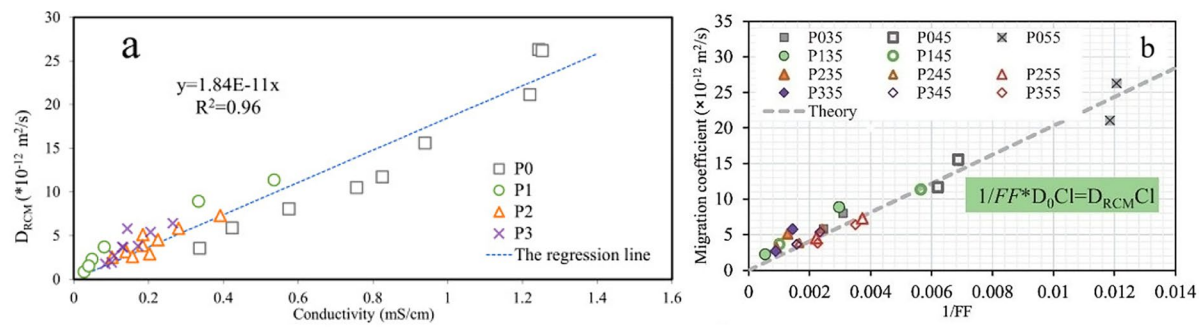

Fig. 7 Huang et al. [156]: Correlation of the D_{nssm} (=D_{RCM}) with conductivity and **b** inverse of formation factor (1/FF [157], where formation factor is the sample conductivity normalized by the conductivity of the bulk pore solution). P035 indicates he w/b, e.g. 0.35), while blended binders include FA (P1), GGBFS (P2), and LL (P3)

surface inhomogeneity, which can significantly affect transport behavior, especially in miniature-scale tests.

Building upon these preparation standards, Table 11 presents a method-specific comparison of the three primary chloride transport test types—Dssd (bulk diffusion), Dssm (steady-state migration), and Dnssm (non-steady-state migration). It provides detailed recommendations tailored to each method's operational principles, including test durations, voltage ranges, solution types, and modeling approaches. Additionally, Table 11 highlights the practical advantages and limitations of using miniature paste-scale testing over conventional mortar or concrete-scale methods. While miniature tests offer benefits such as reduced material use, faster results, and higher sensitivity to binder composition, they may omit critical features such as aggregate-related tortuosity or realistic exposure profiles. Thus, these

Table 8 Comparative analysis of the models in test methods for chloride diffusivity (based on NMR or chloride measurements)

Sect. No	Test Method	Measures	Scale (Duration)	Pros	Cons	Equation 1 corrections
3.1	FG-NMR self-diffusion (Table 3)	Molecular mobility: D_0 *vs* D_{intra}	cm (min)	Fast, molecular, non-invasive, no tracer, Einstein-Nernst model	Sophisticated equipment, in homogenous (ideal) solution or inert porous media, challenges with (para)magnetic impurities	
3.2 & 3.3	NMR, tracer (e.g. HTO): steady state or transient	Isotope conc. (by NMR): D_{ssd} or D_{nssd}	cm (h to days)	Pore structure (D_{eff}), Molecular D_0 and Ionic, pore D_p simple models	Timely and advanced, Intra- and inter-diffusion in ideal solution (Table 3)	$f_p D_0$ (or Fick's 2nd Fleury 2019) [56]
3.1	Steady-state diffusion, (Page 1981) [6]	Cl flux: D_{ssd}	cm (months)	No binding kinetics, concentration dependency	Long duration, not easy to equilibrate, model complexity	$f_\gamma f_f f_E f_p D_0$ model dependent
3.3	Bulk (transient) diffusion, NT Build 443	Cl profile (Table 5): D_{nssd}	cm (> 35 (90)d)	Close to reality (under seawater), total and free Cl should be used	Long duration, curve fitting without guidance, challenges in free Cl measurements	$f_\gamma f_f f_E f_p D_0$ + binding + ∇J_{flux}
3.3	Fick's 2nd + capillary suction: Salt ponding AASHTO T259, 1980 (2.3)	Chloride profile (Table 5): D_{nssd+}	cm (90 days)	Two mechanisms: diffusion & capillary suction	Fitting diffusion error function theory: unclear effects of the two individual mechanisms, Laborious Cl profile measurement [72]	
3.3	Fick's 2nd + water pressure [71]	Cl profile (Table 5): D_{nssd+}	cm (weeks)	Like water permeability, sound theory	Needs special pressure equipment, may damage specimen microstructure [160]	
4.1	Steady migration NT Build 355, NF XP P18-461	Downstream Cl flux: D_{ssm}	cm (weeks)	Simple single species theory [139]	long equilibration time, uncertainty in Cl flux measurements due to Cl_2 gas formation, electrode-specimen surface ΔV drop not considered, requires multi-specie correction factor	
4.1	Truc's [2000] steady migration [133]	Upstream Cl flux: D_{ssm}	cm (days)	Shorter, overcomes many NT build 355 drawbacks	Single species theory, flux may not be constant and depends on chloride binding	
4.2	NT Build 492 or Tang's [1996] transient migration [112]	Cl penetration depth: D_{nssm}	cm (24–72 h)	Shortest, simple measurement and calculation	Single species theory, colorimetric method not always accurate, ΔV drop needs correction, Cl binding kinetics not considered	
4.2	Breakthrough time transient migration	Cl downstream time delay: D_{nssm}	cm (weeks)	Non-steady state method	Long, theory unclear; multiple definitions of breakthrough time delay [161]	
4.2	Andrade's fitting transient migration [149]	Cl profile (Table 5): D_{nssm}	cm (day)	Analogue diffusion theory: error function	Laborious Cl profile measurement, Diffusion theory limitations	
4.2	Equivalent time transient migration [162]	Cl profile: D_{nssm}	cm (day)	Steady state analytical solution	Requires correlation with natural diffusion tests	

Table 9 Comparative analysis of diffusion and migration methods with suitability for paste applications

Category	Test Method	Pros	Cons	Suitability for Paste
Diffusion Methods	Steady-State Diffusion (D_{ssd})	Direct and theoretically sound measurement of D_{eff} No transient effects thin and homogeneous paste samples	Thin samples sensitive to cracks Challenging to perform with large or heterogeneous samples	Accurate for intrinsic $D_{eff}(c)$ under controlled concentration (c) boundary conditions
	Non-Steady-State Diffusion (D_{nssd})	- Best method for chloride diffusivity measurement (realistic conditions) - can be used to study migration during hydration (no cross-section) - Provides comprehensive results for binder behavior and SCM effects	Long test duration (days to months) Complex modeling to separate D_{eff} from binding, if separate equilibrium binding input data available	Realistic conditions. Most relevant and accurate, but requires precise input for binding equilibrium
Migration Methods	Steady-State Migration (D_{ssm})	- Relatively quick test duration - Measures chloride flux directly - Applicable to damaged samples - Applicable to paste samples	- Equilibration challenging - Not field-relevant - Assumes single species theory - Cracks	Good for controlled experiments, limited field relevance; linear correlation with bulk conductivity
	Non-Steady-State Migration (D_{nssm})	- Relatively fast test duration (hours to days) - Applicable to concrete and paste scale	- Mostly single species theory - Binding equilibrium not fully accounted for - Requires accurate chloride flux measurements	Suitable for rapid testing but limited by model assumptions Limited relation to D_{eff} & D_{app}: requires validation with D_{nssd}; Linear correlation with normalised bulk conductivity

Table 10 Cement paste sample preparation guidelines for miniature diffusivity and migration tests

Parameter	Recommendation	Rationale/Notes
Pre-mix Blended Powders	Use two-stage water addition and vacuum mixing	Enhances homogeneity and reduces entrapped air
Water Quality	Use deaired, deionised or demineralised water	Prevents impurities and air bubbles
Water-to-Binder Ratio	Avoid high w/b ratios prone to bleeding	Prevents segregation and ensures uniform microstructure
Bleeding Control	Rotate samples during curing; delayed mixing	Minimizes bleeding, promotes early flocculation
Sample preparation	Avoid core sampling; Polish or cut surface layers	Removes inhomogeneous zones near cast surfaces
Curing Method	Minimal water sealed curing or sacrificial slurry	Reduces leaching while maintaining internal hydration
Curing Duration	Prefer longer curing ($\geq$ 28 days) for less reactive SCMs (91 or 180 days, 1 year)	Promotes stable microstructure and reliable diffusion measurement
Coating Preparation	Apply epoxy/polyurethane on all faces except exposure (only one basal surface coated for D_{ssd})	Ensures one-dimensional diffusion path during testing
Pre-exposure conditioning	Re-saturate samples if drying occurred	Prevents chloride ingress by advection

Table 11 Recommendations for miniature diffusion and migration testing on cement pastes

Parameter	D_{ssd} (Bulk Diffusion)	D_{ssm}	D_{nssm}	Rationale / Notes
Sample size	Cylindrical (D = 33 or 63 mm; H = 10 mm) or Rectangular parallelepipeds (150*200*15 mm^3)	Cylindrical: D = 33 or 63 mm; H = 10 mm	Cylindrical: D = 22 – 55 mm; H ~ 50 mm	Ensure sample homogeneity, reduce cracking, size consistency
Pre-exposure conditioning	Re-saturate samples if drying occurred after coating	Re-saturation required	Re-saturation recommended	Prevents chloride ingress by advection (consistency)
Reservoir/ Exposure Solution	3–3.9% NaCl (seawater), ~0.1 M Cl^- (groundwater)	500 mM NaCl + 300 mM NaOH upstream; 300 mM NaOH downstream	10% NaCl upstream; 0.3 M NaOH downstream	Standardizes ionic environment; controls electrode reactions
Reservoir Volume / Size	Maintain 50 cm^2/L solution-to-surface ratio (ASTM C1556)	≥ 100 mL per cell; steady chloride gradient	3.5 or 12 L catholyte and 20 or 300 mL anolyte	Controls leaching; maintains ion equilibrium
Voltage / Current	Not applicable	5–12 V (avoid overheating); ~300 V/m field strength	30–40 V initial voltage; controlled to avoid damage	Excessive voltage causes damage
Test Duration	up to 28 days	1–3 weeks (commonly ~ 14 days)	~24 h	Paste downscaling accelerates testing
Temperature Control	20–25 °C typical; maintain it stable (e.g., 20 ± 2 °C); Temperature effects identified as interesting research direction			Temperature affects ion mobility and reactions
Coating	Epoxy on all but exposed face	Epoxy coating of lateral sides		unidirectional Cl^- ingress
Measurement Frequency	Single (or multiple) timepoint post exposure chloride profils (three replicates)	Frequent voltage/current and ≤ daily downstream chloride monitoring	Multiple profile depth points (2 minimum; 4–5 preferred)	Calculation of D *'s* for pastes follow same eq. used for concrete samples
Chloride Profiling	Powder titration or High-resolution (SEM–EDS, μXRF, etc.; see Table 4); Total (and 'free') chlorides	Optional if relying on electrical data	Simplified profiles; fewer points suffice for paste-scale	Balances accuracy and test duration; challenges in free chloride detection
Modeling Approach	Square root law (Xcr/$\sqrt{t}$); Fick's Law for D_{app}	Andrade's equation for effective diffusion from steady current	Transient migration models; time-dependent migration rates	Each requires method-specific modelling, Single-specie theory limit
Common Challenges	Bleeding, drying shrinkage, leaching	Electrode interface degradation; solution renewal	Interface dissolution; current damage, Cl binding uncertainty	Handling and electrical conditions critical; Single-specie theory limitations
SCM Impact Assessment	SCMs affect diffusion coefficient and chloride binding	'D_{eff}' correlates with bulk conductivity; distinguishes pore vs solution effects	D_{nssm} correlates well with concrete; pore refinement ↓D_{nssm}	Useful for SCM optimization and durability prediction

Table 11 (continued)

Parameter	D_{ssd} (Bulk Diffusion)	D_{ssm}	D_{nssm}	Rationale / Notes
Pros (of using miniature tests)	Speedup (week to month); Realistic diffusion conditions; Provides comprehensive results for binder behaviour and SCM effects; Most relevant and accurate (compared to migration) tests)	Relatively fast test duration (week); Measures chloride flux directly; Applicable to damaged (paste) samples; linear correlation with bulk conductivity	Fastest test duration (1 day); Fast screening of SCMs' effect; small sample size allows high throughput; linear correlation with normalised bulk conductivity	Low material usage; Faster test duration under; Clear sensitivity to SCMs; Minimal leaching in small sealed systems;
Cons (of using miniature tests)	Paste-scale to mortar/concrete correlations still missing; Complex modelling to separate D_{eff} from Cl-binding (require separate equilibrium binding tests);	Artificial field conditions; single specie theory limitations; Time dependent flux; binding effects	High voltage may distort results; Interface damage risk; Simplified conditions vs. real concrete	No aggregate effects; May underrepresent tortuosity and ITZ; Less realistic for service-life predictions

comparative insights from Table 11 support informed test selection and interpretation in research and durability assessment contexts.

5.2 Main findings

Based on this literature review, the following key insights can be synthesized:

- Diffusion varies by type, with ionic diffusion being the most complex. Key factors include concentration, molecular size, interactions, and ionic strength.
- PFG NMR efficiently measures self-diffusion but is limited by sensitivity to paramagnetic impurities and early hydration stages. It can eliminate binding artifacts and accurately assess pore structures.
- NMR concentration measurements, though not widely available, provide reliable insights into diffusion, porosity, and microstructure in cementitious materials.
- Traditional HTO-through diffusion methods are closest to the fundamental effective diffusion coefficients (D_{eff}), but are time-consuming, leading to exploration of alternative methods.
- The bulk diffusion transient test protocol mimics real-world conditions (without acceleration of diffusion) and provides an engineering D_{app} approach that lumps contributions from both microstructure and chloride binding, although not being an intrinsic property as it varies with boundary and test conditions. The common interpretation approach to fit chloride profiles with an analytical solution of Fick's second law (considering linear binding and constant surface concentration) to obtain D_{app} is criticized due to some hypotheses and the evolution of D_{app} with time (possibly corrected in engineering approaches with an aging factor).
- To speed up the determination of $D_{app}(t)$, an alternative empirical approach is provided (fib Bulletin 34, 2006 [52]; Model Code 2010 [154] based on chloride migration tests D_{nssm}, which should always incorporate a calibration factor to account for the correlation with $D_{app}(t)$ [68, 154].
- An alternative interpretation that has gained attention in recent years is the square root law of diffusion, which seems to describe very well the evolution of chloride penetration depths (with an offset

when samples are exposed before microstructure stabilization).
- Bulk diffusion transient testing has been successfully tested at the paste scale, with the advantage of down-scaling the specimens without aggregates, allowing for greater precision and easier understanding of mechanisms. However, the casting and curing of cement pastes require special precautions because their properties are much more sensitive to inhomogeneity, bleeding, drying shrinkage, and leaching.
- Several methods allow chloride profile measurements in solid phases, each offering different levels of precision (e.g. single point analysis with colorimetry vs. profiles with < 1mm resolution vs. high resolution spectroscopic techniques) and complexity (availability of instrument, sample preparation, possibility of quantitative measurements, complexity of calibration, etc.). Variable pressure SEM–EDS seems to be a promising approach as it allows quantitative profiles with a relatively simple instrument and without extensive sample preparation.

Although there is a growing interest in durability of blended cements, this review highlights that there remain many open questions on methodology how to obtain diffusion coefficients. From this study, it is concluded that the following areas of research require further investigation:

- Various models with different inputs and diffusion coefficient definitions require careful calibration and validation, integrating thermodynamics, kinetics, and microstructure to optimize cement chemistry, though separating the underlying processes remains challenging.
- Adapt NMR for materials with higher paramagnetic impurities, develop cost-effective setups, and expand its focus to inter-diffusion. Standardizing sample preparation and exploring advanced techniques for pore size and anisotropy analysis could enhance understanding of microstructural influences on diffusion.
- Extended studies on a broader range of cementitious materials (concrete, mortar, and paste) are needed to evaluate the limits of the square root diffusion law approach for profile analysis.
- A clearer distinction is needed between moderate chloride concentrations (e.g., marine environments) and high chloride concentrations (e.g., deicing salts with stronger binding effects).
- Laboratory test methods should better account for continuous leaching effects (e.g., marine exposure), as chloride ingress is influenced by hydroxyl leaching.
- Despite numerous bulk diffusion tests on cement paste, a standardized experimental protocol and repeatability studies are still lacking.
- Comprehensive bulk diffusion testing, alongside mortar and concrete assessments, is necessary to evaluate the representativeness of paste results.
- Further research is needed to quantify how SCM-driven reductions in porosity, changes in capillary pore morphology, and increases in C(A)SH density individually impact D reduction.
- The effect of SCMs on the C_d value—often assumed constant in migration tests—should be reconsidered to more accurately assess D_{nssm} in concretes with SCMs.

Acknowledgements The authors would like to thank all members of the RILEM TC 298-EBD for valuable discussions.

Funding Open Access funding enabled and organized by Projekt DEAL.

Data availability All data generated and analyzed during this study are included in this manuscript.

References

1. Ukrainczyk N, Ukrainczyk V (2008) A neural network method for analysing concrete durability. Mag Concr Res 60(7):475–486. https://doi.org/10.1680/macr.2007.00016
2. Shi X, Xie N, Fortune K, Gong J (2012) Durability of steel reinforced concrete in chloride environments: an overview. Constr Build Mater 30:125–138. https://doi.org/10.1016/j.conbuildmat.2011.12.038
3. Wilson W, Georget F, Scrivener KL (2024) Towards a two-step assessment of the chloride ingress behaviour of new cementitious binders. Cem Concr Res 184:107594. https://doi.org/10.1016/j.cemconres.2024.107594
4. Nestle N, Galvosas P, Kärger J (2007) Liquid-phase self-diffusion in hydrating cement pastes — results from NMR studies and perspectives for further research. Cem Concr Res 37(3):398–413. https://doi.org/10.1016/j.cemconres.2006.02.004
5. Fleury M, Berthe G, Chevalier T (2018) Diffusion of water in industrial cement and concrete. Magn Reson Imaging 56:32–36. https://doi.org/10.1016/j.mri.2018.09.010
6. Page CL, Short NR, El Tarras A (1981) Diffusion of chloride ions in hardened cement pastes. Cem Concr Res 11(3):395–406. https://doi.org/10.1016/0008-8846(81)90111-3
7. ASTM C1556 - 11a, Standard test method for determining the apparent chloride diffusion coefficient of cementitious mixtures by bulk diffusion 1," 2016. [Online]. Available: www.astm.org
8. NT BUILD 443:1995, "Concrete, Hardened: accelerated chloride penetration", [Online]. Available: www.nordtest.org
9. ISO 1920–11:2013, "Testing of concrete - Part 11: determination of the chloride resistance of concrete, unidirectional diffusion
10. EN 12390–11:2015, Testing hardened concrete—Part 11: determination of the chloride resistance of concrete, unidirectional diffusion
11. Vennesland M-ACCA (2013) Recommendation of RILEM TC 178-TMC: testing and modelling chloride penetration in concrete*. Mater Struct 46(3):337–344. https://doi.org/10.1617/s11527-012-9968-1
12. RILEM TC 178-TMC, Analysis of water soluble chloride content in concrete," Mater Struct, 35(9) 586–588, Nov. 2002, 10.1007/BF02483129
13. RILEM TC 178-TMC, Analysis of total chloride content in concrete," *Mater Struct*, vol. 35, no. 9, pp. 583–585, Nov. 2002, doi: 10.1007/BF02483128
14. NT BUILD 355 – Edition 2, Concrete, mortar and cement based repair materials: Chloride diffusion coefficient from migration cell experiments, Nov. 1997
15. XP P 18–461, "Concrete — Chloride migration of hardened concrete in Steady State, French standards, AFNOR, 2012
16. NT BUILD 492, "NT BUILD 492 CONCRETE, Mortar and cement-based repair materials: chloride migration coefficient from non-steady-state migration experiments, 1999
17. XP P 18–462, "Concrete—chloride migration of hardened concrete in non steady state, French standards, AFNOR," 2012
18. EN 12390–18, "Testing hardened concrete - Part 18: Determination of the chloride migration coefficient.".
19. UNE 83987:2014, "Concrete durability. Test methods. Measurement of chloride diffusion coefficient in hardened concrete. Multiregime method," p. 20, Jul. 2014
20. UNE 83992–2:2012 EX, Durability of concrete. Test methods. Chloride penetration tests on concrete. Part 2: Integral accelerated method, Oct. 2012
21. Koenders E, Imamoto K, Soive A (eds) (2022) Benchmarking chloride ingress models on real-life case studies—marine submerged and road sprayed concrete structures, vol 37. Springer International Publishing, Cham
22. De Weerdt K, Wilson W, Machner A, Georget F (2023) Chloride profiles – what do they tell us and how should they be used? Cem Concr Res 173:107287. https://doi.org/10.1016/j.cemconres.2023.107287
23. Meng Z, Liu Q, Ukrainczyk N, Mu S, Zhang Y, De Schutter G (2024) Numerical study on the chemical and electrochemical coupling mechanisms for concrete under combined chloride-sulfate attack. Cem Concr Res 175:107368. https://doi.org/10.1016/j.cemconres.2023.107368
24. Elakneswaran Y, Iwasa A, Nawa T, Sato T, Kurumisawa K (2010) "Ion-cement hydrate interactions govern multi-ionic transport model for cementitious materials." Cem Concr Res 40(12):1756–1765. https://doi.org/10.1016/j.cemconres.2010.08.019
25. Hosokawa Y, Yamada K, Johannesson B, Nilsson LO (2011) Development of a multi-species mass transport model for concrete with account to thermodynamic phase equilibriums. Mater Struct/Materiaux et Construct 44(9):1577–1592. https://doi.org/10.1617/s11527-011-9720-2
26. Jensen MM, De Weerdt K, Johannesson B, Geiker MR (2015) Use of a multi-species reactive transport model to simulate chloride ingress in mortar exposed to NaCl solution or sea-water. Comput Mater Sci 105:75–82. https://doi.org/10.1016/j.commatsci.2015.04.023
27. Soive A, Ukrainczyk N, Koenders E (2022) Marine submerged. In: Ki EI, Koenders S, (Eds.) Benchmarking chloride ingress models on real-life case studies—marine submerged and road sprayed concrete structures, RILEM STAR Reports., vol. 37, Springer, Cham., 2022, pp. 25–57. doi: 10.1007/978–3–030–96422–1_3.
28. Shafikhani M, Chidiac SE (2019) Quantification of concrete chloride diffusion coefficient – a critical review. Cem Concr Compos 99:225–250. https://doi.org/10.1016/j.cemconcomp.2019.03.011
29. Tong L, Liu Q, Xiong Q, Meng Z, Amiri O, Zhang M (2025) Modeling the chloride transport in concrete from microstructure generation to chloride diffusivity prediction. Comput-Aided Civil Infrastruct Eng 40(9):1129–1149. https://doi.org/10.1111/mice.13331
30. Othmen I, Bonnet S, Schoefs F (2018) Statistical investigation of different analysis methods for chloride profiles within a real structure in a marine environment. Ocean

Eng 157:96–107. https://doi.org/10.1016/j.oceaneng.2018.03.040
31. Touil B, Ghomari F, Khelidj A, Bonnet S, Amiri O (2022) Durability assessment of the oldest concrete structure in the Mediterranean coastline: the Ghazaouet harbour. Mar Struct 81:103121. https://doi.org/10.1016/j.marstruc.2021.103121
32. Tang L (1999) Concentration dependence of diffusion and migration of chloride ions. Cem Concr Res 29(9):1463–1468. https://doi.org/10.1016/S0008-8846(99)00121-0
33. Ukrainczyk N, Koenders E (2023) Calibration of Tang's model for concentration dependence of diffusion in cementitious materials. In: Jędrzejewska A, Kanavaris F, Azenha M, Benboudjema F, Schlicke D (Eds.), pp. 667–678. 10.1007/978-3*031-33211-1_60
34. Zhang Y, Di Luzio G, Alnaggar M (2021) Coupled multi-physics simulation of chloride diffusion in saturated and unsaturated concrete. Constr Build Mater 292:123394. https://doi.org/10.1016/j.conbuildmat.2021.123394
35. Samson E, Marchand J, Beaudoin JJ (1999) Describing ion diffusion mechanisms in cement-based materials using the homogenization technique. Cem Concr Res 29(8):1341–1345. https://doi.org/10.1016/S0008-8846(99)00101-5
36. Revil A (1999) Ionic diffusivity, electrical conductivity, membrane and thermoelectric potentials in colloids and granular porous media: a unified model. J Colloid Interface Sci 212(2):503–522. https://doi.org/10.1006/jcis.1998.6077
37. van Brakel J, Heertjes PM (1974) Analysis of diffusion in macroporous media in terms of a porosity, a tortuosity and a constrictivity factor. Int J Heat Mass Transf 17(9):1093–1103. https://doi.org/10.1016/0017-9310(74)90190-2
38. Ukrainczyk N, Koenders EAB (2014) Representative elementary volumes for 3D modeling of mass transport in cementitious materials. Model Simul Mater Sci Eng 22(3):035001. https://doi.org/10.1088/0965-0393/22/3/035001
39. Patel RA et al (2016) Diffusivity of saturated ordinary Portland cement-based materials: a critical review of experimental and analytical modelling approaches. Cem Concr Res. https://doi.org/10.1016/j.cemconres.2016.09.015
40. Snyder KA (2001) The relationship between the formation factor and the diffusion coefficient of porous materials saturated with concentrated electrolytes: theoretical and experimental considerations
41. Spragg R, Qiao C, Barrett T, Weiss J (2016) Assessing a concrete's resistance to chloride ion ingress using the formation factor. In: Corrosion of steel in concrete structures, Elsevier, pp. 211–238. 10.1016/B978-1-78242-381-2.00011-0.
42. Georget F, Wilson W, Matschei T (2023) Long-term extrapolation of chloride ingress: an illustration of the feasibility and pitfalls of the square root law. Cem Concr Res 170:107187. https://doi.org/10.1016/j.cemconres.2023.107187
43. Baroghel-Bouny V, Kinomura K, Thiery M, Moscardelli S (2011) Easy assessment of durability indicators for service life prediction or quality control of concretes with high volumes of supplementary cementitious materials. Cem Concr Compos 33(8):832–847. https://doi.org/10.1016/j.cemconcomp.2011.04.007
44. Delagrave A, Bigas JP, Ollivier JP, Marchand J, Pigeon M (1997) Influence of the interfacial zone on the chloride diffusivity of mortars. Adv Cem Based Mater 5(3–4):86–92. https://doi.org/10.1016/S1065-7355(96)00008-9
45. Xi Y, Bažant ZP (1999) Modeling chloride penetration in saturated concrete. J Mater Civ Eng 11(1):58–65. https://doi.org/10.1061/(ASCE)0899-1561(1999)11:1(58)
46. Soive A, Baroghel-Bouny V (2012) Influence of gravel distribution on the variability of chloride penetration front in saturated uncracked concrete. Constr Build Mater 34:63–69. https://doi.org/10.1016/j.conbuildmat.2012.02.060
47. Liu Q, Cai Y, Peng H, Meng Z, Mundra S, Castel A (2023) A numerical study on chloride transport in alkali-activated fly ash/slag concretes. Cem Concr Res 166:107094. https://doi.org/10.1016/j.cemconres.2023.107094
48. Isgor OB, Weiss WJ (2019) A nearly self-sufficient framework for modelling reactive-transport processes in concrete. Mater Struct/Materiaux et Construct. https://doi.org/10.1617/s11527-018-1305-x
49. Martín-Pérez B, Zibara H, Hooton RD, Thomas MDA (2000) "A study of the effect of chloride binding on service life predictions." Cem Concr Res 30(8):1215–1223. https://doi.org/10.1016/S0008-8846(00)00339-2
50. Wilson W, Gonthier JN, Georget F, Scrivener KL (2022) Insights on chemical and physical chloride binding in blended cement pastes. Cem Concr Res 156:106747. https://doi.org/10.1016/j.cemconres.2022.106747
51. Thomas MDA, Hooton RD, Scott A, Zibara H (2012) The effect of supplementary cementitious materials on chloride binding in hardened cement paste. Cem Concr Res 42(1):1–7. https://doi.org/10.1016/j.cemconres.2011.01.001
52. Schiessl P et al. (2006) fib Bulletin 34. Model Code for Service Life Design. fib. In: The international federation for structural concrete. 10.35789/fib.BULL.0034
53. Dhandapani Y et al (2024) Performance of cementitious systems containing calcined clay in a chloride-rich environment: a review by TC-282 CCL. Mater Struct 57(7):154. https://doi.org/10.1617/s11527-024-02426-7
54. Andrade C, Castellote M, d'Andrea R (2011) Measurement of ageing effect on chloride diffusion coefficients in cementitious matrices. J Nucl Mater 412(1):209–216. https://doi.org/10.1016/j.jnucmat.2010.12.236
55. Attari A, McNally C, Richardson MG (2016) A probabilistic assessment of the influence of age factor on the service life of concretes with limestone cement/GGBS binders. Constr Build Mater 111:488–494. https://doi.org/10.1016/j.conbuildmat.2016.02.113
56. Fleury M, Berthe G, Chevalier T (2019) Diffusion of water in industrial cement and concrete. Magn Reson Imaging 56:32–36. https://doi.org/10.1016/j.mri.2018.09.010
57. Hansen EW, Gran HC, Johannessen E (2005) Diffusion of water in cement paste probed by isotopic exchange experiments and PFG NMR. Microporous Mesoporous

Mater 78(1):43–52. https://doi.org/10.1016/j.micromeso.2004.09.015
58. Fleury M, Chevalier T, Berthe G, Dridi W, Adadji M (2020) Water diffusion measurements in cement paste, mortar and concrete using a fast NMR based technique. Constr Build Mater 259:119843. https://doi.org/10.1016/j.conbuildmat.2020.119843
59. Valori A, McDonald PJ, Scrivener KL (2013) The morphology of C-S–H: lessons from ^{1}H nuclear magnetic resonance relaxometry. Cem Concr Res 49:65–81. https://doi.org/10.1016/j.cemconres.2013.03.011
60. Luraschi P, Gimmi T, Van Loon LR, Shafizadeh A, Churakov SV (2020) Evolution of HTO and 36Cl− diffusion through a reacting cement-clay interface (OPC paste-Na montmorillonite) over a time of six years. Appl Geochem 119:104581. https://doi.org/10.1016/j.apgeochem.2020.104581
61. Larbi B, Dridi W, Dangla P, Le Bescop P (2016) Link between microstructure and tritiated water diffusivity in mortars: impact of aggregates. Cem Concr Res 82:92–99. https://doi.org/10.1016/j.cemconres.2016.01.003
62. Pel L, Ji Y, Zhang X, Kurvers M, Sun Z (2025) Non-destructive measurement of chloride profiles in cementitious materials using NMR. J Nondestr Eval 44(1):9. https://doi.org/10.1007/s10921-024-01139-9
63. Ziehensack E, Keßler S, Angst U, Hilbig H, Gehlen C (2023) Diffusion potentials in saturated hardened cement paste upon chloride exposure. Mater Struct 56(5):100. https://doi.org/10.1617/s11527-023-02184-y
64. Castellote M, Alonso C, Andrade C, Chadbourn GA, Page CL (2001) Oxygen and chloride diffusion in cement pastes as a validation of chloride diffusion coefficients obtained by steady-state migration tests. Cem Concr Res 31(4):621–625. https://doi.org/10.1016/S0008-8846(01)00469-0
65. Numata S, Amano H, Minami K (1990) Diffusion of tritiated water in cement materials. J Nucl Mater 171(2–3):373–380. https://doi.org/10.1016/0022-3115(90)90383-X
66. Yang Y, Patel RA, Churakov SV, Prasianakis NI, Kosakowski G, Wang M (2019) Multiscale modeling of ion diffusion in cement paste: electrical double layer effects. Cem Concr Compos 96:55–65. https://doi.org/10.1016/j.cemconcomp.2018.11.008
67. Sammaljärvi J et al (2024) Autoradiographic imaging of the spatial distribution of Cl-36 in concrete. Constr Build Mater 456:139279. https://doi.org/10.1016/j.conbuildmat.2024.139279
68. Carmen A, Moro F, Torrent F, Torrenti J-M, Von Greve-Dierfeld S (2024) Transport of liquids, gases, and ions in hardened concrete, pp. 7–15. 10.35789/fib.BULL.0112.Ch03.
69. Fjendbo S, Sørensen HE, De Weerdt K, Geiker MR (2021) "The square root method for chloride ingress prediction—Applicability and limitations." Mater Struct 54(2):61. https://doi.org/10.1617/s11527-021-01643-8
70. Fraj AB, Bonnet S, Leklou N, Khelidj A (2019) Investigating the early-age diffusion of chloride ions in hardening slag-blended mortars on the light of their hydration progress. Constr Build Mater 225:485–495. https://doi.org/10.1016/j.conbuildmat.2019.07.185
71. Allan Freeze R, Cherry JA Groundwater
72. McGrath PF, Hooton RD (1999) Re-evaluation of the AASHTO T259 90-day salt ponding test. Cem Concr Res 29(8):1239–1248. https://doi.org/10.1016/S0008-8846(99)00058-7
73. Jensen OM, Hansen PF, Coats AM, Glasser FP (1999) Chloride ingress in cement paste and mortar. Cem Concr Res 29(9):1497–1504. https://doi.org/10.1016/S0008-8846(99)00131-3
74. Silva N, Luping T, Rauch S (2013) Application of LA-ICP-MS for meso-scale chloride profiling in concrete. Mater Struct/Materiaux et Construct 46(8):1369–1381. https://doi.org/10.1617/s11527-012-9979-y
75. Wilson W, Georget F, Scrivener K (2021) Unravelling chloride transport/microstructure relationships for blended-cement pastes with the mini-migration method. Cem Concr Res 140:106264. https://doi.org/10.1016/j.cemconres.2020.106264
76. Spragg R, Villani C, Snyder K, Bentz D, Bullard JW, Weiss J (2013) Factors that influence electrical resistivity measurements in cementitious systems. Trans Res Record J Trans Res Board 2342(1):90–98. https://doi.org/10.3141/2342-11
77. Bernard T, Wilson W (2025) Comparison of curing methods for bulk electrical conductivity testing of cement pastes. Mater Struct 58:134. https://doi.org/10.1617/s11527-024-02558-w
78. Elakneswaran Y, Iwasa A, Nawa T, Sato T, Kurumisawa K (2010) Ion-cement hydrate interactions govern multi-ionic transport model for cementitious materials. Cem Concr Res 40(12):1756–1765. https://doi.org/10.1016/j.cemconres.2010.08.019
79. Mejlhede Jensen O, Hansen PF, Coats AM, Glasser FP (1999) Chloride ingress in cement paste and mortar. Cem Concr Res. https://doi.org/10.1016/S0008-8846(99)00131-3
80. Bernard T, Wilson W (2025) Square-root law prediction of chloride penetration rates in stabilized sement pastes. https://doi.org/10.2139/ssrn.5276160
81. Poulsen SL, Sørensen HE (2014) Chloride ingress in old Danish bridges. 10.13140/2.1.3054.7521.
82. Poulsen SL, Sørensen HE, Jönsson U Chloride ingress in concrete blocks at the rødbyhavn marine exposure site-status after 5 years." [Online]. Available: www.expertcentre.dk
83. Wilson W, Georget F, Scrivener KL (2023) XCr/$\sqrt{t}$ as an Indicator of the resistance against bulk chloride diffusion. In: SynerCrete 2023. RILEM Bookseries 43. Springer.https://doi.org/10.1007/978-3-031-33211-1_59
84. Wilson W, Georget F, Scrivener KL (2023) The square root law with an offset applied to chloride diffusion in slowly reacting blended cement pastes. In: ICCC2023
85. Georget F, Wilson W, Matschei T (2023) Impact of an evolving microstructure on the square-root law for chloride ingress. In: ICCC2023
86. Georget F, Babaahmadi A, Machner A, Mrak M, Dolenec S, Xiang Xiong Q, Shiju J, Snoeck D, Suraneni P & Wilson W (2025) Measuring chloride binding in cementitious materials: a review by RILEM TC 298-EBD. Mater Struct [In print]

87. Shafikhani M, Chidiac SE Relationships between free and water-soluble chloride concentrations in concrete
88. Bonnet S, Schoefs F, Salta M (2020) Sources of uncertainties for total chloride profile measurements in concrete: quantization and impact on probability assessment of corrosion initiation. Eur J Environ Civil Eng 24(2):232–247. https://doi.org/10.1080/19648189.2017.1375997
89. Khanzadeh Moradllo M et al (2017) Using micro X-ray fluorescence to image chloride profiles in concrete. Cem Concr Res 92:128–141. https://doi.org/10.1016/j.cemconres.2016.11.014
90. Trejo D, Ahmed AA (2019) Adopting auto-titration to assess chlorides in concrete. ACI Mater J. https://doi.org/10.14359/51715580
91. Otsuki N, Nagataki S, Nakashita K (1993) Evaluation of the AgNO3 solution spray method for measurement of chloride penetration into hardened cementitious matrix materials. Constr Build Mater. https://doi.org/10.1016/0950-0618(93)90002-T
92. Fu C, Li S, He R, Zhou K, Zhang Y (2022) Chloride profile characterization by electron probe microanalysis, powder extraction and AgNO3 colorimetric: a comparative study. Constr Build Mater. https://doi.org/10.1016/j.conbuildmat.2022.127892
93. He F, Shi C, Yuan Q, An X, Tong B (2011) Calculation of chloride concentration at color change boundary of AgNO3 colorimetric measurement. Cem Concr Res 41(11):1095–1103. https://doi.org/10.1016/j.cemconres.2011.06.008
94. Achenbach R, Raupach M (2024) Suitability of rapid chloride migration tests for determining the migration coefficient in mortars made from different novel binder types. Mater Corros 75(9):1173–1184. https://doi.org/10.1002/maco.202414369
95. He F, Shi C, Yuan Q, Chen C, Zheng K (2012) AgNO3-based colorimetric methods for measurement of chloride penetration in concrete. Constr Build Mater 26(1):1–8. https://doi.org/10.1016/j.conbuildmat.2011.06.003
96. Baroghel-Bouny V, Belin P, Maultzsch M, Henry D (2007) AgNO3 spray tests: advantages, weaknesses, and various applications to quantify chloride ingress into concrete. Part 1: Non-steady-state diffusion tests and exposure to natural conditions. Mater Struct. https://doi.org/10.1617/s11527-007-9233-1
97. Peterson K, Julio-Betancourt G, Sutter L, Hooton RD, Johnston D (2013) Observations of chloride ingress and calcium oxychloride formation in laboratory concrete and mortar at 5°C. Cem Concr Res 45:79–90. https://doi.org/10.1016/j.cemconres.2013.01.001
98. Dempere LMB, Willenberg R Deist , and University of Florida. College of Engineering. In: Use of scanning electron microscopy and microanalysis to determine chloride content of concrete and raw materials." [Online]. Available: https://rosap.ntl.bts.gov/view/dot/26278
99. Jensen OM, Coats AM, Glasser FP (1996) Chloride ingress profiles measured by electron probe micro analysis. Cem Concr Res 26(11):1695–1705. https://doi.org/10.1016/S0008-8846(96)00158-5
100. Mori D, Yamada K, Hosokawa Y, Yamamoto M (2006) Applications of electron probe microanalyzer for measurement of Cl concentration profile in concrete. J Adv Concr Technol 4(3):369–383. https://doi.org/10.3151/jact.4.369
101. Pacheco J, Çopuroğlu O (2016) quantitative energy-dispersive X-ray microanalysis of chlorine in cement paste. J Mater Civil Eng 28(1):04015065. https://doi.org/10.1061/(ASCE)MT.1943-5533.0001336
102. Jenneson PM, Clough AS, Hollands R, Mulheron MJ, Jeynes C (1998) Profiling chlorine diffusion into ordinary Portland cement and pulverized fuel ash pastes using scanning MeV proton micro-PIXE. J Mater Sci Lett 17(14):1173–1175. https://doi.org/10.1023/A:1006508820103
103. Bernard T, Wilson W (2025) Simplified Chloride ingress quantification using SEM-EDS and the square root law in cement pastes. https://doi.org/10.2139/ssrn.5511583
104. Wilsch G, Weritz F, Schaurich D, Wiggenhauser H (2005) Determination of chloride content in concrete structures with laser-induced breakdown spectroscopy. Constr Build Mater 19(10):724–730. https://doi.org/10.1016/j.conbuildmat.2005.06.001
105. Völker T, Gottlieb C, Kapteina G, Wilsch G, Millar S, Reichling K (2024) Neues DGZfP-Merkblatt B14: Quantifizierung von Chlorid in Beton mittels LIBS. Beton-Stahlbetonbau 119(7):529–535. https://doi.org/10.1002/best.202400014
106. Völker T et al (2023) Interlaboratory comparison for quantitative chlorine analysis in cement pastes with laser induced breakdown spectroscopy. Spectrochim Acta B Atom Spectrosc 202:106632. https://doi.org/10.1016/j.sab.2023.106632
107. Millar S, Gottlieb C, Günther T, Sankat N, Wilsch G, Kruschwitz S (2018) Chlorine determination in cement-bound materials with laser-induced breakdown spectroscopy (LIBS) – a review and validation. Spectrochim Acta B At Spectrosc 147:1–8. https://doi.org/10.1016/j.sab.2018.05.015
108. Völker T, Mensing FM, Kruschwitz S (2025) Estimation of cement content in concrete by spatially resolved laser induced breakdown spectroscopy. Cem Concr Res 189:107714. https://doi.org/10.1016/j.cemconres.2024.107714
109. Gottlieb C, Millar S, Grothe S, Wilsch G (2017) 2D evaluation of spectral LIBS data derived from heterogeneous materials using cluster algorithm. Spectrochim Acta Part B At Spectrosc 134:58–68. https://doi.org/10.1016/j.sab.2017.06.005
110. Pourbozorgi Langroudi P, Kapteina G, Illguth M (2021) Automated distinction between cement paste and aggregates of concrete using laser-induced breakdown spectroscopy. Materials 14(16):4624. https://doi.org/10.3390/ma14164624
111. Millar S, Kruschwitz S, Wilsch G (2019) Determination of total chloride content in cement pastes with laser-induced breakdown spectroscopy (LIBS). Cem Concr Res 117:16–22. https://doi.org/10.1016/j.cemconres.2018.12.001
112. Gottlieb C, Millar S, Günther T, Wilsch G (2017) Revealing hidden spectral information of chlorine and sulfur in data of a mobile laser-induced breakdown spectroscopy system using chemometrics. Spectrochim Acta Part B At

Spectrosc 132:43–49. https://doi.org/10.1016/j.sab.2017.04.001
113. Eto S, Matsuo T, Matsumura T, Fujii T, Tanaka MY (2014) Quantitative estimation of carbonation and chloride penetration in reinforced concrete by laser-induced breakdown spectroscopy. Spectrochim Acta B 101:245–253. https://doi.org/10.1016/j.sab.2014.09.004
114. Burakov VS, Kiris VV, Raikov SN (2007) Optimization of conditions for spectral determination of chlorine content in cement-based materials. J Appl Spectrosc 74(3):321–327. https://doi.org/10.1007/s10812-007-0052-5
115. Wakil MA, Alwahabi ZT (2019) Microwave-assisted laser induced breakdown molecular spectroscopy: quantitative chlorine detection. J Anal At Spectrom 34(9):1892–1899. https://doi.org/10.1039/C9JA00151D
116. Khanzadeh Moradllo M, Hu Q, Ley MT (2017) "Using X-ray imaging to investigate in-situ ion diffusion in cementitious materials." Constr Build Mater 136:88–98. https://doi.org/10.1016/j.conbuildmat.2017.01.038
117. Climent MA, Viqueira E, de Vera G, López-Atalaya MM (1999) Analysis of acid-soluble chloride in cement, mortar, and concrete by potentiometric titration without filtration steps. Cem Concr Res 29(6):893–898. https://doi.org/10.1016/S0008-8846(99)00063-0
118. BW and Luisa RD, Dempere A, (2013) Use of scanning electron microscopy and microanalysis to determine chloride content of concrete and raw materials
119. Gottlieb C, Günther T, Wilsch G (2018) Impact of grain sizes on the quantitative concrete analysis using laser-induced breakdown spectroscopy. Spectrochim Acta B At Spectrosc 142:74–84. https://doi.org/10.1016/j.sab.2018.02.004
120. Silva N, Luping T, Rauch S (2013) Application of LA-ICP-MS for meso-scale chloride profiling in concrete. Mater Struct 46(8):1369–1381. https://doi.org/10.1617/s11527-012-9979-y
121. Khanzadeh Moradllo M, Hu Q, Ley MT (2017) Using X-ray imaging to investigate in-situ ion diffusion in cementitious materials. Constr Build Mater 136:88–98. https://doi.org/10.1016/j.conbuildmat.2017.01.038
122. Standard method of test for rapid determination of the chloride permeability of concrete. *Washington D.C*
123. Whiting D (1981) Rapid determination of the chloride ion permeability of concrete-FHWA-RD-81–119," Washington, D.C
124. Dhir RK, Jones MR, Ahmed HEH, Seneviratne AMG (1990) Rapid estimation of chloride diffusion coefficient in concrete. Mag Concr Res 42(152):177–185
125. Tang L, Nilsson L-O (1992) Rapid determination of chloride diffusivity of concrete by applying an electrical field. ACI Mater J 49:49–53
126. Andrade C (1993) Calculation of chloride diffusion coefficients in concrete from ionic migration measurements. Cem Concr Res 23(3):724–742. https://doi.org/10.1016/0008-8846(93)90023-3
127. NF XP P18–461, (2012) Test on hardened concrete: accelerated test of chloride ions in Steady State, determination of the effective diffusion coefficient of chloride ions, French standard, France
128. Tang L (1996) Electrically accelerated methods for determining chloride diffusivity in concrete—current development. Mag Concr Res 48(176):173–179. https://doi.org/10.1680/macr.1996.48.176.173
129. Andrade C, Sanjuán MA, Recuero A, Río O (1994) Calculation of chloride diffusivity in concrete from migration experiments, in non steady-state conditions. Cem Concr Res 24(7):1214–1228. https://doi.org/10.1016/0008-8846(94)90106-6
130. Djerbi A, Bonnet S, Khelidj A, Baroghel-bouny V (2008) Influence of traversing crack on chloride diffusion into concrete. Cem Concr Res 38(6):877–883. https://doi.org/10.1016/j.cemconres.2007.10.007
131. Djerbi Tegguer A, Bonnet S, Khelidj A, Baroghel-Bouny V (2013) Effect of uniaxial compressive loading on gas permeability and chloride diffusion coefficient of concrete and their relationship. Cem Concr Res 52:131–139. https://doi.org/10.1016/j.cemconres.2013.05.013
132. Hauck CJ (1993) The effect of curing temperature and silica fume on chloride migration and pore structure of high strength concrete. University of Trondheim, The Norwegian Institute of Technology
133. Truc O, Ollivier JP, Carcassès M (2000) A new way for determining the chloride diffusion coefficient in concrete from steady state migration test. Cem Concr Res 30(2):217–226. https://doi.org/10.1016/S0008-8846(99)00232-X
134. Castellote M, Andrade C, Alonso C (2001) Measurement of the steady and non-steady-state chloride diffusion coefficients in a migration test by means of monitoring the conductivity in the anolyte chamber. Comparison with natural diffusion tests. Cem Concr Res 31(10):1411–1420. https://doi.org/10.1016/S0008-8846(01)00562-2
135. Cherif R, Andrade C, Aït-Mokhtar A, Hamami AE-A (2023) On the calculation of chloride diffusion coefficient from the multispecies transference numbers in the standard migration test. Cem Concr Res 167:107133. https://doi.org/10.1016/j.cemconres.2023.107133
136. Hemstad P, Machner A, De Weerdt K (2020) The effect of artificial leaching with HCl on chloride binding in ordinary Portland cement paste. Cem Concr Res 130:105976. https://doi.org/10.1016/j.cemconres.2020.105976
137. Tang L, Nilsson L-O, Basheer PAM (2011) Resistance of concrete to chloride ingress. CRC Press. https://doi.org/10.1201/b12603
138. Samson E, Marchand J, Snyder KA (2003) Calculation of ionic diffusion coefficients on the basis of migration test results. Mater Struct 36(3):156–165. https://doi.org/10.1007/BF02479554
139. Zhang T, Gjørv OE (1995) Effect of ionic interaction in migration testing of chloride diffusivity in concrete. Cem Concr Res 25(7):1535–1542. https://doi.org/10.1016/0008-8846(95)00147-5
140. Zhang T, Gjørv OE (1994) An electrochemical method for accelerated testing of chloride diffusivity in concrete. Cem Concr Res 24(8):1534–1548. https://doi.org/10.1016/0008-8846(94)90168-6
141. Truc O (2000) Prediction of chloride penetration into saturated concrete—multi—species approach

142. Friedmann H, Amiri O, Aït-Mokhtar A, Dumargue P (2004) A direct method for determining chloride diffusion coefficient by using migration test. Cem Concr Res 34(11):1967–1973. https://doi.org/10.1016/j.cemconres.2004.01.009
143. Krabbenhøft K, Krabbenhøft J (2008) Application of the Poisson–Nernst–Planck equations to the migration test. Cem Concr Res 38(1):77–88. https://doi.org/10.1016/j.cemconres.2007.08.006
144. Aït-Mokhtar A, Amiri O, Poupard O, Dumargue P (2004) A new method for determination of chloride flux in cement-based materials from chronoamperometry. Cem Concr Compos 26(4):339–345. https://doi.org/10.1016/S0958-9465(03)00008-8
145. Hu Y, Xiong L, Yan Y, Geng G (2024) Performance of limestone calcined clay cement (LC3) incorporating low-grade marine clay. Case Stud Constr Mater 20:e03283. https://doi.org/10.1016/j.cscm.2024.e03283
146. Wilson W, Georget F, Scrivener K (2021) Unravelling chloride transport/microstructure relationships for blended-cement pastes with the mini-migration method. Cem Concr Res. https://doi.org/10.1016/j.cemconres.2020.106264
147. Pontes J, Bogas JA, Real S, Silva A (2021) The rapid chloride migration test in assessing the chloride penetration resistance of normal and lightweight concrete. Appl Sci 11(16):7251. https://doi.org/10.3390/app11167251
148. Guignone GC, Vieira GL, Zulcão R, Mion G, Baptista G (2019) Analysis of the chloride diffusion coefficients by different test methods in concrete mixtures containing metakaolin and high-slag blast-furnace cement. Matéria (Rio de Janeiro). https://doi.org/10.1590/s1517-707620190004.0837
149. Andrade C, Castellote M, Alonso C, González C (2000) "Non-steady-state chloride diffusion coefficients obtained from migration and natural diffusion tests. Part I: Comparison between several methods of calculation." Mater Struct 33(1):21–28. https://doi.org/10.1007/BF02481692
150. Spiesz P, Ballari MM, Brouwers HJH (2012) RCM: a new model accounting for the non-linear chloride binding isotherm and the non-equilibrium conditions between the free- and bound-chloride concentrations. Constr Build Mater 27(1):293–304. https://doi.org/10.1016/j.conbuildmat.2011.07.045
151. Tang L, Sørensen HE (2001) Precision of the Nordic test methods for measuring the chloride diffusion/migration coefficients of concrete. Mater Struct 34(8):479–485. https://doi.org/10.1007/BF02486496
152. Bagheri AR, Zanganeh H (2012) Comparison of rapid tests for evaluation of chloride resistance of concretes with supplementary cementitious materials. J Mater Civ Eng 24(9):1175–1182. https://doi.org/10.1061/(ASCE)MT.1943-5533.0000485
153. Andrade C (1993) Calculation of chloride diffusion coefficients in concrete from ionic migration measurements. Cem Concr Res. https://doi.org/10.1016/0008-8846(93)90023-3
154. fib MC 2010, The fib model code for concrete structures 2010
155. fib bulletin 76:2015, Benchmarking of deemed-to-satisfy provisions in standards - durability of reinforced concrete structures exposed to chlorides
156. Huang L, Tang L, Löfgren I, Olsson N, Yang Z (2022) Real-time monitoring the electrical properties of pastes to map the hydration induced microstructure change in cement-based materials. Cem Concr Compos 132:104639. https://doi.org/10.1016/j.cemconcomp.2022.104639
157. Huang L, Tang L, Löfgren I, Olsson N, Yang Z, Li Y (2022) Moisture and ion transport properties in blended pastes and their relation to the refined pore structure. Cem Concr Res 161:106949. https://doi.org/10.1016/j.cemconres.2022.106949
158. Ranger M, Hasholt MT (2023) Relationship between chloride migration, bulk electrical conductivity and formation factor of blended cement pastes. Nordic Concr Res 69(2):33–53. https://doi.org/10.2478/ncr-2023-0009
159. EL Achrafi MK, Bonnet S, Villain G (2023) Electrical resistivity tomography results analyzed with two inversion methods to determine chloride profiles on BFS concrete having very high electrical resistivity. Constr Build Mater 407:133361. https://doi.org/10.1016/j.conbuildmat.2023.133361
160. Stanish KD, Hooton RD, Thomas MDA Testing the chloride penetration resistance of concrete: a literature review
161. Halamickova P, Detwiler RJ, Bentz DP, Garboczi EJ (1995) Water permeability and chloride ion diffusion in portland cement mortars: Relationship to sand content and critical pore diameter. Cem Concr Res 25(4):790–802. https://doi.org/10.1016/0008-8846(95)00069-O
162. Castellote M, Andrade C, Alonso C (2001) Non-steady-state chloride diffusion coefficients obtained from migration and natural diffusion tests. Part II: different experimental conditions. Joint relations. Mater Struct 34(6):323–331. https://doi.org/10.1007/BF02486483
163. Sergi G, Yu SW, Page CL (1992) Diffusion of chloride and hydroxyl ions in cementitious materials exposed to a saline environment. Mag Concr Res 44(158):63–69. https://doi.org/10.1680/macr.1992.44.158.63
164. Baroghel-Bouny V, Wang X, Thiery M, Saillio M, Barberon F (2012) Prediction of chloride binding isotherms of cementitious materials by analytical model or numerical inverse analysis. Cem Concr Res 42(9):1207–1224. https://doi.org/10.1016/j.cemconres.2012.05.008
165. Sui S, Georget F, Maraghechi H, Sun W, Scrivener K (2019) Towards a generic approach to durability: factors affecting chloride transport in binary and ternary cementitious materials. Cem Concr Res 124:105783. https://doi.org/10.1016/j.cemconres.2019.105783